



Mohamed Khider University of Biskra
Faculty of exact sciences and natural and life sciences
Material sciences department

MASTER MEMORY

Material Sciences
Physics
Physics of materials

Ref. :

Presented by:
Baara Meriem

Simulation of the effect of quantum wells on light-emitting diodes

Jury :

Dr. Afak Meftah	Professor	University Biskra	President
Dr. Toufik Tibermacine	Professor	University Biskra	Supervisor
Dr. Ouahiba Boudib	M.C.A	University Biskra	Examiner

Academic year: 2022/2023

Dedication

Praise be to God who helped me for doing this humble job.

To who sacrificed every time for me, "Mom, sweetheart of my heart."

To my "wonderful father", who has always supported me.

"God cared for and preserved them"

To my family who always stood by my "brothers and sisters"

*And to everyone who left an imprint, even if simple, during my
academic career.*

Meriem

Thanks and appreciation

*I would like first to thank God, who gave me strength and patience to
achieve This work.*

*I extend my sincere thanks and gratitude to my Supervisor
Professor "J. Tibermacine" for his follow-up, advice and guidance
throughout the search.*

*I also extend my sincere thanks and appreciation to those who have
helped and assisted, in particular, Professor "R. Boumaraf"*

*I would also like to thank my distinguished teachers for their
acceptance of the discussion of this note and their valuable corrections
and guidance.*

Abstract

Using the SILVACO software, we have simulated the effect of quantum wells on the electrical and optical characteristics of MQWs light emitting diodes. The quantum wells InGaN are inserted at the junction between n-GaN and p-GaN. In an ideal case, electrons of type n diffuse towards the conduction band of the quantum wells. Similarly, holes coming from the p-type diffuse towards the valence band of the quantum wells. The carriers then locate themselves in the wells. As carrier densities n and p are large in the wells. Radiation recombination becomes faster than non-radiative recombination, so the efficiency of the device is increased. In addition, the oscillation force is large in a quantum well, which also leads to an increase in the efficiency of the LED in comparison to that of a homo-junction or hetero-junction. Nevertheless, due to the increasing series resistance, a larger number of wells would bring a higher turn-on voltage. In addition, the interface of MQWs would become rougher with increase of wells number, and deteriorate the emission efficiency. Therefore, it is proposed that the interface of MQWs should be taken into account when exploring the optimal QWs number to obtain high performance InGaN/GaN LEDs.

Key words: Light emitting diodes, InGaN/GaN, Quantum wells, Simulation, SILVACO-ATLAS.

المخلص

باستخدام برنامج SILVACO، قمنا بمحاكاة تأثير الآبار الكمومية على الخصائص الكهربائية والبصرية للتنائيات الباعثة للضوء MQWs. يتم إدخال الآبار الكمومية InGaN بين n-GaN و p-GaN في الحالة المثالية، تنتشر الإلكترونات من النوع n باتجاه نطاق التوصيل للآبار الكمومية. وبالمثل، تنتشر الثقوب القادمة من النوع p باتجاه نطاق التكافؤ في الآبار الكمومية. ثم تتمركز الحاملات في الآبار الكمومية. نظرًا لأن كثافات الناقلات n و p كبيرة في الآبار. يصبح الالتحام الإشعاعي أسرع من الالتحام غير الإشعاعي، وبالتالي تزداد كفاءة التنائيات الباعثة. بالإضافة إلى ذلك، فإن قوة الاهتزاز كبيرة في البئر الكمي، مما يؤدي أيضًا إلى زيادة كفاءة LED مقارنةً بكفاءة الوصلة المتجانسة أو الوصلة غير المتجانسة. ومع ذلك، و نظرًا لزيادة المقاومة المتسلسلة، فإن عددًا أكبر من الآبار سيؤدي إلى زيادة جهد التشغيل. بالإضافة إلى ذلك، ستصبح عدد الحدود بين الآبار الكمومية أكثر مع زيادة عدد الآبار، مما يؤدي إلى تدهور كفاءة الانبعاث. لذلك، يُقترح أن تؤخذ عدد الحدود بين الآبار الكمومية في الاعتبار عند البحث عن العدد الأمثل للآبار الكمومية للحصول على تنائيات الباعثة للضوء InGaN / GaN عالية الأداء.

الكلمات المفتاحية: التنائيات الباعثة للضوء، InGaN/GaN، الآبار الكمومية، المحاكاة، SILVACO-ATLAS.

Table of contents

Dedication	I
Thanks and appreciation	II
Abstract	III
Table of contents	IV
List of figures	VII
List of tables	IX
General introduction	1
Chapter I: Basic Concepts on Semiconductors	
I.1.Introduction	2
I.2.Semiconductors	2
I.3.Types of semiconductors	3
I.3.1.Intrinsic semiconductors	3
I.3.2.Extrinsic semiconductors	4
I.3.2.1.Semiconductor type N	4
I.3.2.1.Semiconductor type P	5
I.4.Charge carrier concentration	6
I.5.Direct and indirect semiconductors	7
I.5.1.Direct gap semiconductor	8
I.5.2.Indirect gap semiconductor	8
I.6.Generation–Recombination	9
I.6.1.Generation	9
I.6.2.Recombination	9
I.6.2.1.Radiative recombination	10
I.6.2.2.Auger recombination	10
I.6.2.3.Shockley Read Hall recombination	11
I.6.2.4.Surface recombination	12
I.7.Gallium nitride GaN layer	13
I.8.Indium gallium nitride InGaN layer	13
I.9.Aluminum gallium nitride AlGaN layer	14
I.10.InGaN/GaN quantum wells	14
Chapter II: Light Emitting Diodes	
II.1.Introduction	15

II.2.Definition	15
II.3.PN junction	16
II.3.1.Forward bias of the junction	17
II.3.2.Reverse bias of the junction	18
II.4.Principle of LED operation	19
II.5.Classification of light emitting diodes	20
II.5.1.Structure classification	20
II.5.1.1.Homojunction light emitting diodes	20
II.5.1.2.Heterojunction light emitting diodes	21
II.5.1.3.Quantum well LEDs	22
II.5.2.Power classification	23
II.5.2.1.Low power LED	23
II.5.2.2.High-Power LED	24
II.5.3.Emission spectra classification	25
II.5.3.1.Monochromatic light emitting diodes	25
II.5.3.2.White light emitting diodes	26
II.5.3.3.Infrared light emitting diodes	26
II.6.Properties of light emitting diodes	26
II.6.1.Optical properties	26
II.6.1.1.Quantum efficiencies	26
II.6.1.2.Emission spectra	27
II.6.1.3.Optical power	27
II.6.1.4.Luminous efficiency of light emitting diodes	28
II.6.2.Electrical properties	29
II.7.Applications of LEDs	30
II.8.Advantages and disadvantages of light emitting diodes	30
II.8.1.Advantages	30
II.8.2.Disadvantages	31
Chapter III: SILVACO-ATLAS and simulation results	
III.1.Introduction	32
III.2.Presentation of the SILVACO program package	32
III.2.1.ATLAS	33
III.2.1.1.Deckbuild	34

III.2.1.2.Tonyplot	35
III.2.2.Basic semiconductor equations in ATLAS-SILVACO	35
III.2.3.Syntax of a program in ATLAS	36
III.2.3.1.Mesh	36
III.2.3.2.Region	37
III.2.3.3.Electrode	38
III.2.3.4.Doping	39
III.2.4.Specification of material parameters and physical models	40
III.2.4.1.Materials	40
III.2.4.2.Models	40
III.2.5.Selection of the numerical method	41
III.2.6.Solution Specification	41
III.2.6.1.Log	41
III.2.6.2.Solve	41
III.2.6.3.Save	42
III.2.7.Analyse of results	42
III.2.7.1.EXTRACT	42
III.2.7.2.TONYPLOT	42
III.3.Simulation results	43
III.3.1.Representation of the simulated structure	43
III.3.2.Simulation parameters of the LED	45
III.3.3.Current-Voltage characteristic	46
III.3.4.Spectral power	47
III.3.5.Luminous Power	48
III.3.6.Spectral power of 2QWs at different voltages	49
III.3.7.Internal quantum efficiency	50
III.3.8. Comparison of ordinary and multiple quantum well light-emitting diodes	52
General conclusion	54
References	

List of figures

Figure I.1:	Representation of energy bands.	2
Figure I.2:	Si doping with Arsenic As: N-type semiconductor.	5
Figure I.3:	Grafting Si with Bore B: P-type semiconductor.	6
Figure I.4:	A schematic of the difference between a direct gap and an indirect gap.	8
Figure I.5:	Direct and indirect transmission of the semiconductor.	9
Figure I.6:	Diagram of the different recombinations mechanisms.	10
Figure I.7:	Auger recombination mechanism. Excess energy from recombination can be transferred to an electron (a) or a hole (b).	11
Figure I.8:	Schokley-Read-Hall recombination mechanism.	12
Figure I.9:	Energy gap and visible spectrum for various semiconductors.	13
Figure I.10:	InGaN/GaN quantum well.	14
Figure II.1:	Representation of a PN junction.	17
Figure II.2:	Forward bias junction.	18
Figure II.3:	Reverse bias junction.	19
Figure II.4:	A schematic illustration of typical planar surface emitting LED devices.	20
Figure II.5:	Structure of a homo-junction LED.	21
Figure II.6:	Schematic diagram of a p-n hetero-junction with three types of semiconductors	22
Figure II.7:	Quantum well LEDs.	23
Figure II.8:	Architecture of a low power LED.	23
Figure II.9:	Architecture of a high power LED.	24
Figure II.10:	LED voltage current characteristic.	29
Figure III.1:	Input and output information types of the ATLAS simulator.	33
Figure III.2:	Deckbuild interface.	34
Figure III.3:	Tonyplot window.	35
Figure III.4:	Mesh definition with Atlas.	37
Figure III.5:	Regions with defined materials.	38
Figure III.6:	Electrode definition.	39
Figure III.7:	Distribution of doping in the regions.	40

Figure III.8:	Diagram of the simulated structure.	44
Figure III.9:	Structure of the multiple quantum well LED.	45
Figure III.10:	I-V characteristics of MQW LED for different number of quantum well.	46
Figure III.11:	Power spectral for different quantum well LED.	47
Figure III.12:	Luminous power for different quantum well.	49
Figure III.13:	The power spectral of 2QWs for different bias voltage.	50
Figure III.14:	Internal quantum efficiency (IQE) as function of number of wells.	51
Figure III.15:	I-V characteristics of SQM and 2QWs.	52
Figure III.16:	Variation of Luminescent power versus anode current.	53

List of tables

Table I.1:	Portion of the periodic table related to semiconductors.	3
Table I.2:	Chemical properties of aluminum gallium nitride.	14
Table II.1:	The different families of light emitting diodes.	25
Table II.2:	Luminous efficiencies of different light source.	28
Table II.3:	Some of the applications of the various families of LEDs.	30

General introduction

Today, a new lighting source is available to reduce electricity consumption such as white light emitting diodes (LEDs) because their energy efficiency, their reliability compared to incandescent bulbs [1]. High-intensity LEDs (HIDs) are currently used in a variety of products, including road signs, automobile headlights, and lamps for home lighting. The InGaN currently stands out as most promising material for visible light emission. Since the development of blue LEDs based on quantum wells in InGaN, the fabrication of good white light sources with high light efficiency has surged [2].

In this work, we will study the effect of number of the number of the quantum wells as well as the effect of bias voltage on the light emitting diode characteristics using SILVACO-ATLAS simulation software. Therefore, this manuscript is composed of three chapters, which are organized as follows: the first chapter introduces briefly the semiconductors, in terms of structures, types and recombination mechanisms. The second chapter is devoted to the study of light-emitting diodes in terms of operating principle, characteristics, classifications, advantages and disadvantages. The third chapter contains two parts, the first part we will introduce the SILVACO simulation software, its modules and simulation tools. In the second part we will study by simulating on one hand, the effect of the number of quantum wells on the electrical and optical properties of the simulated LED and on other hand, the effect of the bias voltage on the optical properties of the simulated LED. Finally, we will end this work with a general conclusion in which we summarize the different obtained results.

Chapter I

Basic Concepts on Semiconductors

I.1.Introduction

Solids can be classified into three sets: insulators, semiconductors and conductors. Insulators are materials with a specified electrical conductivity $\sigma < 10^{-8} \text{S.cm}^{-1}$ (for diamonds is $10^{-14} \text{S.cm}^{-1}$) and semiconductors whose specific electrical conductivity are in range $10^{-8} \text{S.cm}^{-1} < \sigma < 10^3 \text{S.cm}^{-1}$, (for silicon between 10^{-5}S.cm^{-1} and 10^3S.cm^{-1}), the conductors are materials with high specific electrical conductivity (silver, for example, with its specific connectors 10^6S.cm^{-1}) [3, 4].

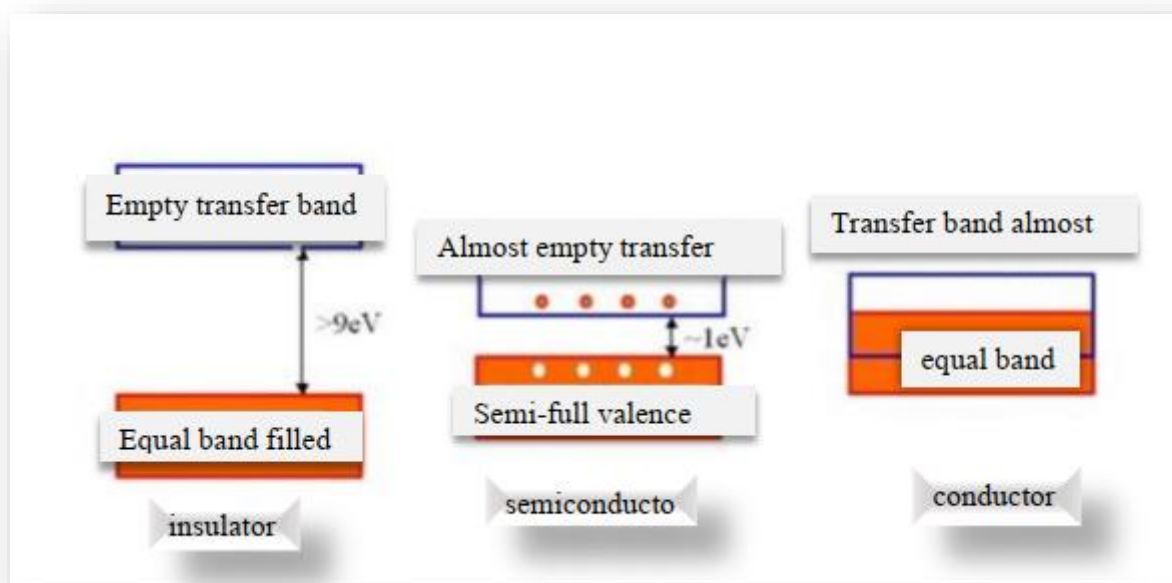


Figure I.1: Representation of energy bands [4].

I.2.Semiconductors

Semiconductors are probably the most significant of the three types of materials in electrical engineering. The conductivity of semiconductors can be dramatically changed in a variety of ways, which makes them special [5, 6]. Despite the fact that there are many distinct types of compound semiconductors, they are often made of two, three, or four different elements and are hence known as binary, ternary, or quaternary compounds, respectively. The Periodic Table's Column III and Column V elements serve as the foundation for the most significant compound semiconductors. These substances are referred to as III-V compound

semiconductors. Gallium arsenide (GaAs), indium phosphate (InP), aluminum arsenide (AlAs), indium arsenide (InAs), and others are examples of III-V compounds. Table I.1 shows a portion of the periodic table related to semiconductors [7].

Period	Column II	III	IV	V	VI
2		B Boron	C Carbon	N Nitrogen	O Oxygen
3	Mg Magnesium	Al Aluminum	Si Silicon	P Phosphorus	S Sulfur
4	Zn Zinc	Ga Gallium	Ge Germanium	As Arsenic	Se Selenium
5	Cd Cadmium	In Indium	Sn Tin	Sb Antimony	Te Tellurium
6	Hg Mercury		Pb Lead		

Table I.1: Portion of the periodic table related to semiconductors [7].

I.3.Types of semiconductors

A semiconductor is a material whose electrical conductivity falls between that of an insulator and a conductor. Semiconductors are classified into two categories: intrinsic and extrinsic semiconductors.

I.3.1.Intrinsic semiconductors

A semiconductor material in its pure form is known as an intrinsic semiconductor. Thus, the intrinsic semiconductors are chemically pure, i.e. they are free from impurities. In case of intrinsic semiconductors, the number of charge carriers (holes and electrons) are determined by the properties of the semiconductor material itself instead of the impurity. Also, the number of free holes is equal to the number of free electrons in the intrinsic semiconductor. The familiar examples of the intrinsic semiconductors are silicon (Si), germanium (Ge) and gallium arsenide (GaAs) [8].

I.3.2.Extrinsic semiconductors

The extrinsic semiconductor is known as doped semiconductor i.e when a little amount of chemical impurity is added to an intrinsic semiconductor. The process of adding impurity in the intrinsic semiconductor is called doping with the aim of increasing the electrical conductivity of semiconductors. Based on the type of doping, the extrinsic semiconductors are classified into two types: P-type semiconductors and N-type semiconductors. When the hole concentration exceeds the electron concentration in a semiconductor that has been doped with acceptors, the semiconductor is referred to as being P-type. Similar to this, if the semiconductor is doped with donors, it is termed to be N-type because the electron concentration is higher than the hole concentration. It is required to compare the hole and electron concentrations with the intrinsic concentration in order to determine if a semiconductor is p-type or n-type. This requires invoking the charge neutrality using the following equation [5]:

$$p - n + N_d^+ - N_a^- = 0 \quad (\text{I.1})$$

I.3.2.1.Semiconductor type N

When a tetravalent atom such as Si is doped with a pentavalent atom, it occupies the position of an atom in the crystal lattice of the Si atom. The four of the electrons of the pentavalent atom bond with the four neighboring silicon atoms, and the fifth one remains weakly bound to the parent atom. As a result, the ionization energy necessary to set the fifth electron free is very small, and the electrons become free to move in the lattice of the semiconductor. Such semiconductors are called as N-type semiconductors.

Figure I.2 shows the introduction of an Arsenic atom in place of Si atoms and the formation of a free electron from the excess electrons. So the electrons in this type are the carriers of the majority charge, and holes are also called the minority charge. A semiconductor doped by donor atoms is called N-type semiconductor.

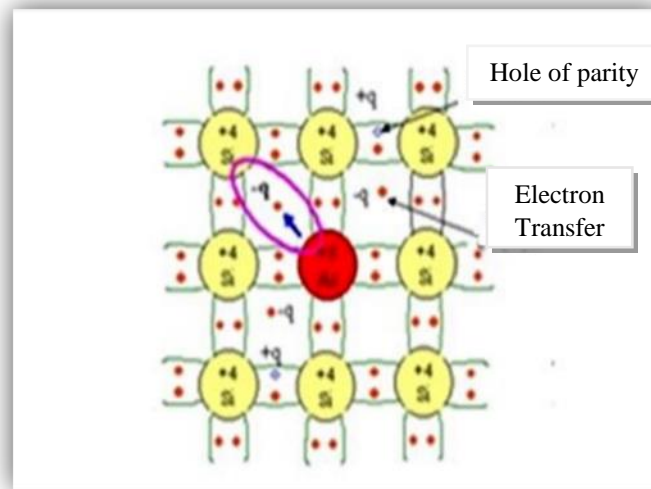


Figure I.2: Si doping with Arsenic: N-type semiconductor.

I.3.2.2.Semiconductor type P

When a tetravalent atom such as Si is doped with a trivalent impurity such as Al, B, In, the doping atom has one less electron than the neighboring atoms of Si. Thus, the fourth atom of the tetravalent atom is free, and a hole is generated in the trivalent atom. In such materials, the holes are the charge carriers, and such semiconductors are termed P-type semiconductors.

Figure (I.3) shows the introduction of a Bore atom in place of Si atoms and the formation of a free hole from the excess holes. So the holes in this type are the carriers of the majority charge, and electrons are also called the minority charge. A semiconductor doped by acceptor atoms is called P-type semiconductor.

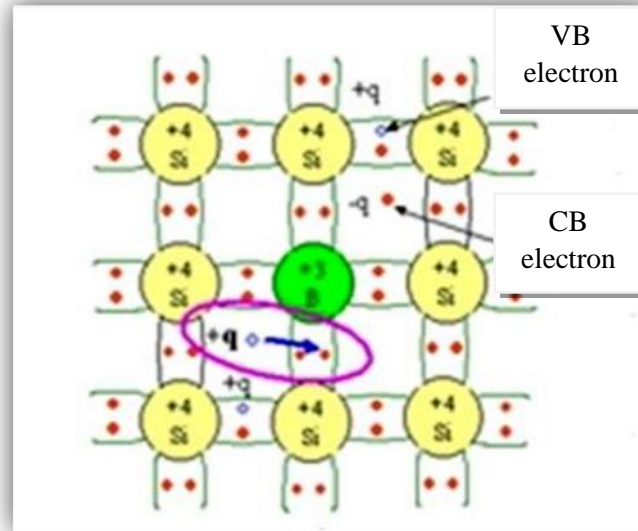


Figure I.3: Doping Si with Bore B: P-type semiconductor.

I.4.Charge carrier concentration

It is necessary to know the concentration of charge carriers in semiconductors if we want to determine their electrical properties. In order to obtain an equation that gives the density of the carriers of the charge, the distribution of these carriers must be known. To that end, statistical methods must be applied and an appropriate distribution function used. To calculate the density of electrons and holes, we use a Fermi distribution function, which gives the probability that the energy level available, E , is occupied with an electron at absolute temperature T . It is given by the following relationship:

$$F(E) = \frac{1}{1 + e^{(E - E_F)/KT}} \quad (I.2)$$

K_B : Boltzmann constant $= 1.38 \times 10^{-23} \text{ J / } ^\circ\text{K}$.

E_f : Fermi level energy.

Fermi distribution function can be used to calculate the density of the electron in the conduction band and the density of the hole in the valence band at a given temperature if we know the density $N(E)$. Then the electron density is given by:

$$n = \int_{E_c}^{\infty} f(E)N(E)dE \quad (I.3)$$

The hole density is given by:

$$p = \int_{-\infty}^{E_v} [1 - f(E)] N(E) dE \quad (I.4)$$

We can also determine the electron density in the conduction band as a product of the effective density in E_c and the occupancy function at E_c using the equation (I.5)

$$n = N_c f(E_c) \quad (I.5)$$

In a similar way, we can write hole density in the valence band as a product of the effective density N_v at the end of the E_v and the occupancy function at E_v :

$$p = N_v [1 - f(E_v)] \quad (I.6)$$

The effective density N_c at temperature T is given by:

$$N_c = 2 \left(\frac{2\pi m_n K T}{h^2} \right)^{3/2} \quad (I.7)$$

N_v is also given by:

$$N_v = 2 \left(\frac{2\pi m_h K T}{h^2} \right)^{3/2} \quad (I.8)$$

m_n : effective mass of an electron.

m_h : effective mass of a hole.

h : Planck is constant.

If we assume that the Fermi level falls below the end of the transport band by more than several KT , i.e. $E_c - E_f \ll KT$, then the electron density is given with the relation:

$$n = N_c e^{-(E_c - E_f)/KT} \quad (I.9)$$

If we assume that the Fermi level is located above the end of the valence band by more than several KT , i.e. $E_f - E_v \gg KT$, then the density of holes refers to the relationship:

$$p = N_v e^{-(E_f - E_v)/KT} \quad (I.10)$$

The validity of the relationship can be easily proven:

$$np = n_i^2 \quad (I.11)$$

Where n_i is the density of the intrinsic carriers which is given by the following relation [4]:

$$n_i = \sqrt{N_c N_v} e^{-E_g/2KT} \quad (I.12)$$

I.5. Direct and indirect semiconductors

The band gap represents the minimum energy difference between the bottom of the conduction band and the top of the valence band. Actually, the top of the valence band and the

bottom of the conduction band are not generally at the same value of the electron momentum (Figure I.4). The lifetimes of minority carriers and the optical characteristics of semiconductors are affected by the type of the gap semiconductor [9].

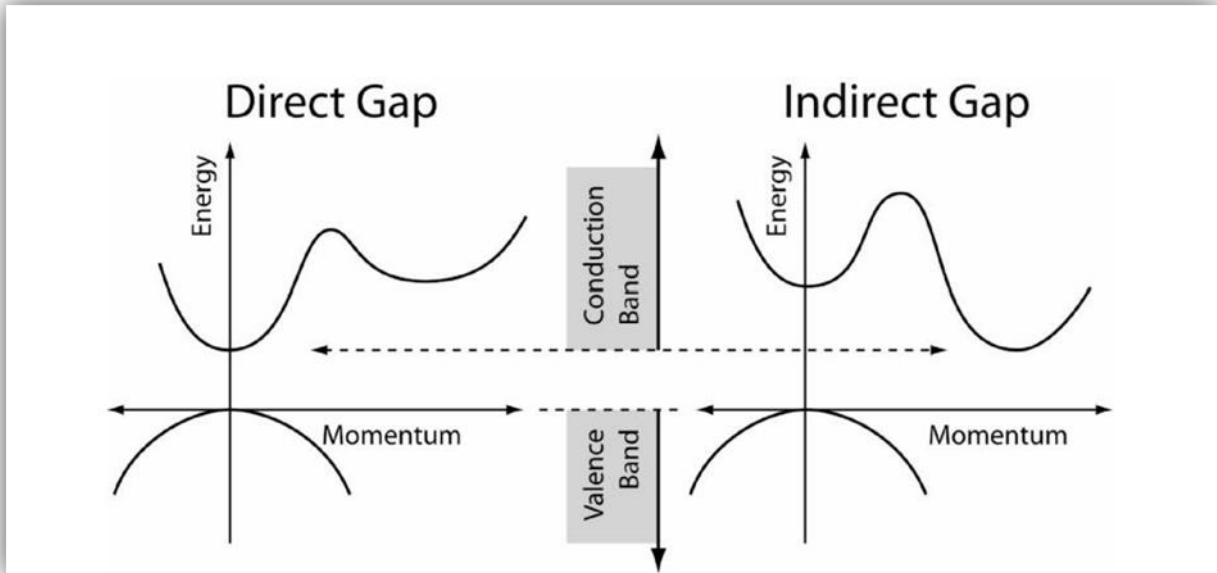


Figure I.4: A schematic of the difference between a direct gap and an indirect gap [9].

I.5.1. Direct gap semiconductor

In a direct band gap semiconductor, the top of the valence band and the bottom of the conduction band occur at the same value of momentum, as shown in the figure (I.5). In semiconductors such as gallium arsenide (GaAs), the bottom (lowest) of the conduction band (where free electrons are found) and the highest valence band have the same value of the wave vector k . The wave vector represents the momentum of carriers as shown in Figure (I.5). The value of this momentum is 0.

I.5.2. Indirect gap semiconductor

In an indirect band gap semiconductor, the maximum energy of the valence band occurs at a different value of momentum to the minimum in the conduction band energy: In silicon and germanium for example, the lower part of the conduction band and the higher part of the valence band have the same values of k it does not happen. This semiconductor is called an

indirect energy gap semiconductor (Figure I.5). This can only happen if an appropriate amount of momentum is transferred to the electron (or hole) while maintaining momentum. This can occur through collisions with one or more phonons [10].

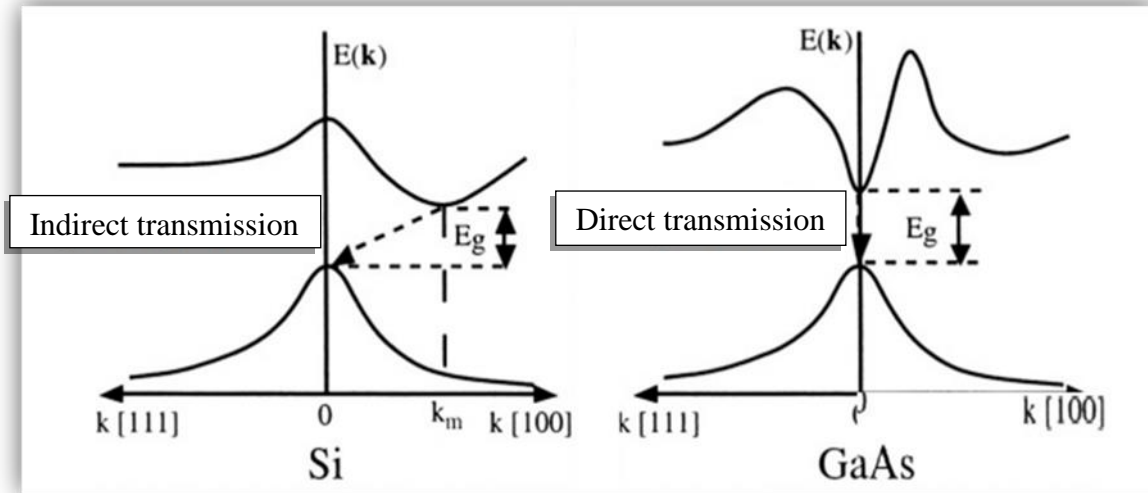


Figure I.5: Direct and indirect transmission of the semiconductor [10].

I.6.Generation–Recombination

I.6.1.Generation

Generation (G) is the creation of carriers in the semiconductor; it is characterized by a parameter that measures the number of carriers created per unit of volume and per unit time ($\text{cm}^{-3}\cdot\text{s}^{-1}$). The generation may be due to thermal agitation or excitation of the semiconductor by an external source (optical, electrical, etc.) [11].

I.6.2.Recombination

Recombination is the inverse phenomenon of generation. The electron loses its energy, either by creating a photon (mainly for materials with a direct band gap) or more generally by returning it to the valence band (heating). Experimentally, the life of minority carrier's τ is measured. This can be determined, for silicon of type p or n, from the rate of recombination R ($\text{cm}^{-3}\cdot\text{s}^{-1}$) by referring to the relation:

$$\tau = \frac{\Delta n}{R} \quad (\text{I.13})$$

Δn (cm^{-3}): representing the excess density of photo-generated (or injected) minority carriers. We will discuss the three fundamental recombination mechanisms: radiative recombination, Auger recombination, and SRH recombination. We will also present surface recombination, which is a special case (Figure (I.6)) [12].

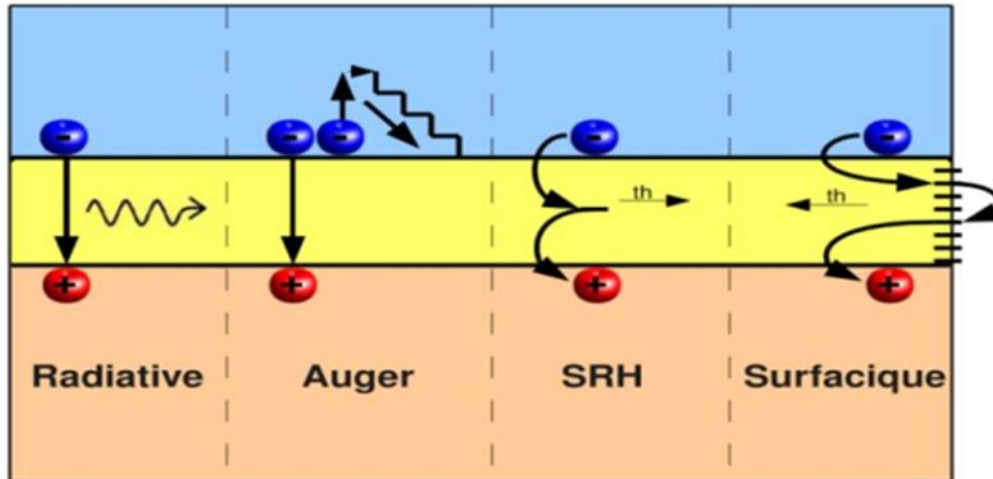


Figure I.6: Diagram of the different recombination mechanisms [12].

I.6.2.1. Radiative recombination

The radiative recombination corresponds to the recombination of an electron of the conduction band with a hole of the valence band, with the emission of a photon of energy close to that of the gap of the material (the reverse process of photo generation). The radiative recombination mechanism is a dominant process in direct-gap semiconductors like GaAs. For silicon with an indirect gap, this mechanism is relatively rare because this transition can only take place with the assistance of a photon [13].

I.6.2.2. Auger recombination

The Auger recombination mechanism is a three-entity mechanism. The excess energy from the recombination of an electron from the conduction band and a hole in the valence band is transferred to a third particle, an electron or a hole. The third particle will then thermalize and release heat. The life time of this mechanism τ_{Aug} is proportional to the

inverse of the squared density of carriers. This mode of recombination will therefore predominate at high levels of injection or doping.

The Auger recombination rate is given by the following expression:

$$R_A = (C_n n + C_p p)(np - n_i^2) \quad (\text{I.14})$$

n_i : is the intrinsic concentration.

C_p and C_n : are the Auger coefficients for holes and electrons.

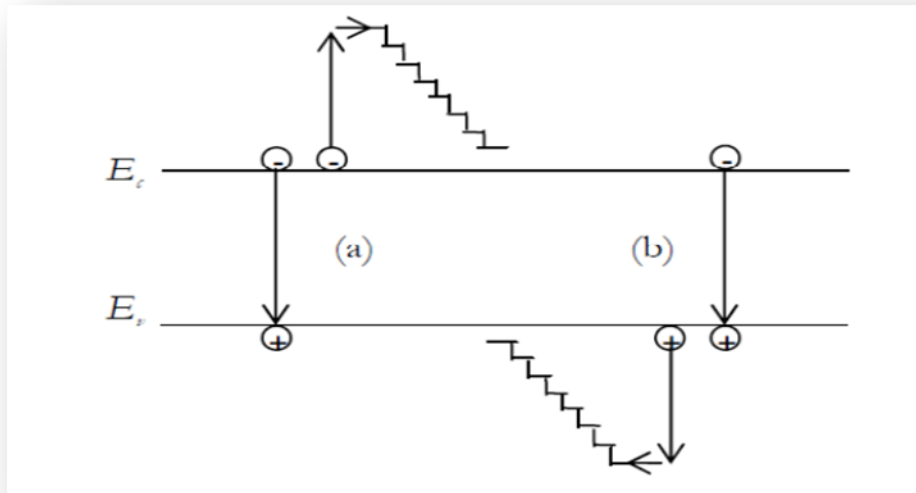


Figure I.7: Auger recombination mechanism. Excess energy from recombination can be transferred to an electron (a) or a hole (b) [13].

I.6.2.3. Shockley Read Hall recombination

Shockley, Read, and Hall first analyzed this recombination process. SRH recombinations are related to the presence of impurities or defects (dislocations, gaps, etc.) within the crystalline structure of silicon and cause a change in the life τ_{SRH} . These defects induce discrete energy levels in the forbidden band of the material, called traps, which facilitate the recombination mechanisms. An electron in the conduction band will first relax at an intermediate energy level. Next, a second relaxation will allow him to recombine with a hole in the valence band. This is the first time that he has had a hole in the valence band [12].

$$R_{SRH} = \frac{pn - n_{ie}^2}{\tau_{p0} [n + n_{ie} \exp(E_{TRAP}/KT)] + \tau_{n0} [p + n_{ie} \exp(-E_{TRAP}/KT)]} \quad (I.15)$$

E_t : is the energy level for the recombination centers.

E_i : is the intrinsic Fermi energy.

E_{TRAP} : is the difference between E_t and E_i .

n_{ie} : is the effective intrinsic carrier concentration including bandgap narrowing effects.

τ_{n0} and τ_{p0} : are respectively the life time for the electrons and holes.

K : is the Boltzmann constant.

T : temperature in Kelvin.

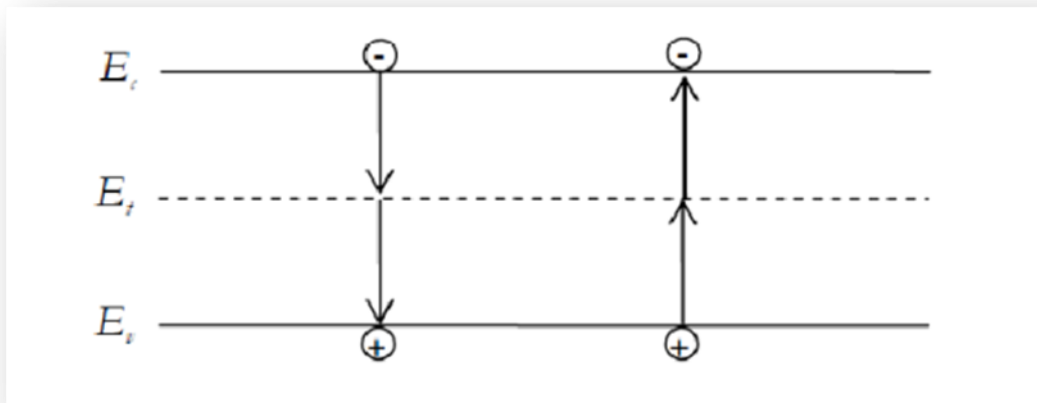


Figure I.8: Schokley-Read-Hall (SRH) recombination mechanism [12].

I.6.2.4. Surface recombination

The surface of a semiconductor is a place where recombination is particularly numerous due to the unsatisfied bonds (dangling bonds) of surface atoms and other characteristic temperature defects ($T = 300$ °K). Front and rear surface recombination inherent in doping densities according to the following relationship [13]:

$$S = S_0 \left(\frac{N}{N_{set}} \right)^\alpha \quad (I-16)$$

I.7. Gallium nitride GaN layer

Any stress exerted on a semiconductor causes a deformation of that solid and, therefore, the position of the atoms relative to each other. If this semiconductor such as GaN, we observe a modification of the dipolar moments of Ga-N bonds linked to the variation of interatomic distances. At 300 K, the GaN gap is 3.4 eV, which corresponds to a wavelength in the near ultraviolet (UV) region of the optical spectrum. The addition of In or Al allows for ternary alloys of InGaN or AlGaN. Depending on the concentration of Al or In, the forbidden band energy can vary from ~0.7 eV (for InN) to ~6.3 eV (for AlN). This covers almost the entire spectrum from red to deep UV. The figure (I. 10) shows the possible variation of the bandwidth of the forbidden GaN by the production of the ternary alloys InGaN and AlGaN. [14].

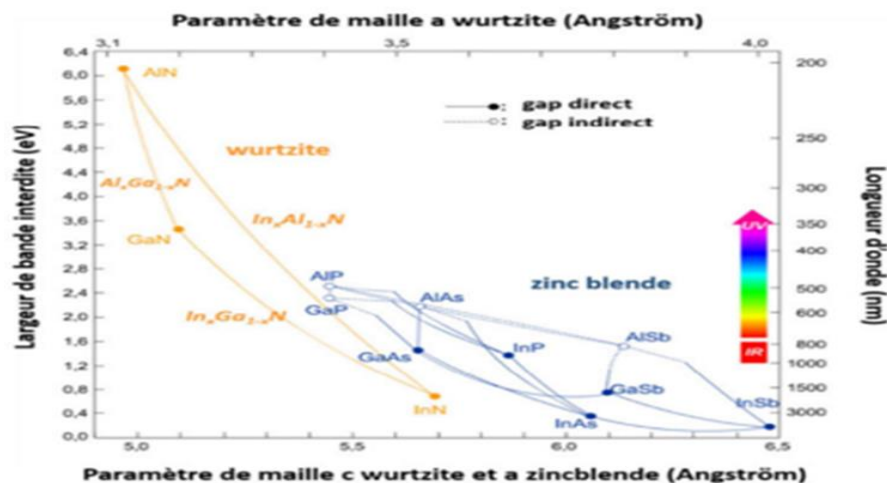


Figure I.9: Energy gap for various semiconductors [14].

I.8. Indium gallium nitride InGaN layer

InGaN currently appears to be the most promising material for the emission of visible light. It is a semiconductor material made of a mixture of gallium nitride (GaN) and indium nitride (InN). Its band gap can be tuned by changing the amount of indium in the alloy. The growth of good-quality InGaN epitaxial layers remains a challenge at this time [2].

I.9. Aluminum gallium nitride AlGaN layer

An alloy of gallium nitride and aluminum nitride is known as aluminum gallium nitride. The AlGaN layer is used to create a hetero-junction with the GaN layer [16]. The chemical properties of aluminum gallium nitride are provided in the table below [15]:

Chemical Properties	
Chemical Formula	AlGaN
Group	Aluminum - 13
	Gallium - 13
	Nitrogen - 15
Lattice Constant	3.17 Å

Table I.2: Chemical properties of aluminum gallium nitride [16].

I.10. InGaN/GaN quantum wells

InGaN/GaN quantum wells occupy a central place in solid state lighting. Quantum wells are inserted at the junction between type n GaN and type p GaN as shown in Figure I.7. In an ideal case, electrons from type n diffuse towards the conduction band of quantum wells, similarly, holes from type p diffuse towards the valence band of quantum wells. Carriers then locate in wells as the densities of carriers n and p are large in wells, radiation recombination becomes faster than non-radiative recombination, so that the efficiency of the device is increased by more, the oscillation force is great in a quantum well [17].

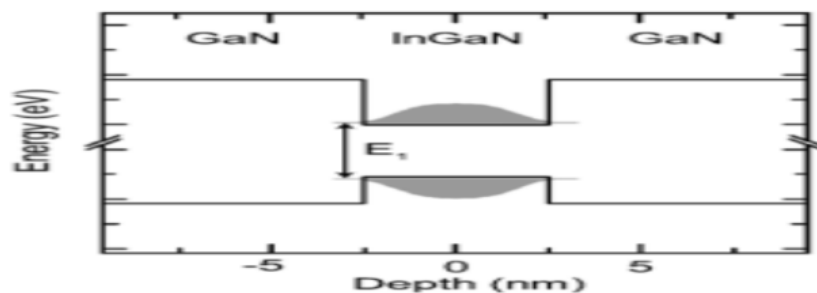


Figure I.10: InGaN/GaN quantum well [17].

Chapter II

Light Emitting Diodes

II.1.Introduction

Light emitting diodes establish themselves as ground-breaking alternatives due to the continual increase in their luminous efficiency [18, 19]. Early in the 1980s, hetero-structures of materials with various energy bandgaps were introduced. Bandgap size of a semiconductor sandwiched between two materials grows by increasing the localization of carriers in the same area and introducing the 2D density of states that characterize quantum confinement in quantum wells [20]. The generalization of the use of light emitting diodes (LED) in the last decade significantly changed the lighting environment of the work. LEDs are present in the news lighting installations or replacement of conventional incandescent or halogen lamps, and mercury vapour. They are also used for the backlight of the screens of all types (computers, tablets, smartphones) [21]. Gallium arsenide phosphate (GaAsP), a novel semiconductor material that was quickly produced, was used to create LEDs. GaAsP has a greater energy gap than GaAs, which results in a shorter wavelength of light. These LEDs initially served only as indicators and provided a red color light [22]. The greatest efficiency of blue SiC LEDs, which produced blue light with a 470 nm wavelength, was only 0.03 percent at the beginning of the 1990s. Due to the limited efficiency of SiC LEDs, however, researchers have begun to focus on other semiconductor materials as a way to improve efficiency and produce light at different frequency ranges. The creation of infrared LEDs based on the use of GaAs was one such method [23].

II.2.Definition

A light emitting diode, abbreviated under the acronyms LED (Light Emitting Diode), is an optoelectronic component capable of emitting light when traversed by an electric current. A light-emitting diode allows the electric current to pass only in one direction and also produces monochromatic or polychromatic light from the conversion of electrical energy when a current passes through it. Their robustness, low consumption and long life time give them indisputable applications. Because of their increasing use, LEDs need to be characterized. This task is not easy since they have spatial and spectral distributions that can differ greatly from one LED to another. In addition, the stability of the output light intensity versus the temperature. For the manufacture of an LED, it is necessary to choose a material with direct transition whose forbidden bandwidth is greater or equal $h\nu$, ν being the frequency

of the radiation emitted. As an example of fabricated LEDs, we can find binary LEDs (AsGa, InP... etc.) or ternary (GaP_xAs_{1-x}, AsIn_xGa_{1-x}... etc.) which cover a region of the spectrum ranging from green (0.55 μm) to far infrared (8.5 μm) [24].

II.3.PN junction

A PN junction is formed to effectively control the electrical characteristics of a material. We know that it allows the passage of the current only in one direction. PN junction consists of two regions respectively doped P and N juxtaposed in a way that we will assume abrupt, that is to say that the transfer of the zone P to the zone N is done abruptly

(Figure II.1). When the two regions are joined together, the difference in concentration between the carriers of the regions P and N will cause the flow of a diffusion current tending to equalize the concentration in carriers from one region to another. The holes in the P region will diffuse towards the N region, leaving behind ionized atoms, which constitute fixed negative charges. The mathematical representation of built in voltage is given by:

$$V_{bi} = \frac{KT}{q} \ln \left[\frac{N_a N_d}{n_i^2} \right] \quad (II.1)$$

Where:

N_a: is the acceptor concentration (cm⁻³).

N_d: is the donor concentration (cm⁻³).

q: is the elementary charge (C).

The width of the depletion region (W) is also related to the level of doping in both regions. It can be calculated using the following equation:

$$W = \left\{ \frac{2\epsilon_s V_{bi}}{e} \left[\frac{N_a + N_d}{N_a N_d} \right] \right\}^{1/2} \quad (II.2)$$

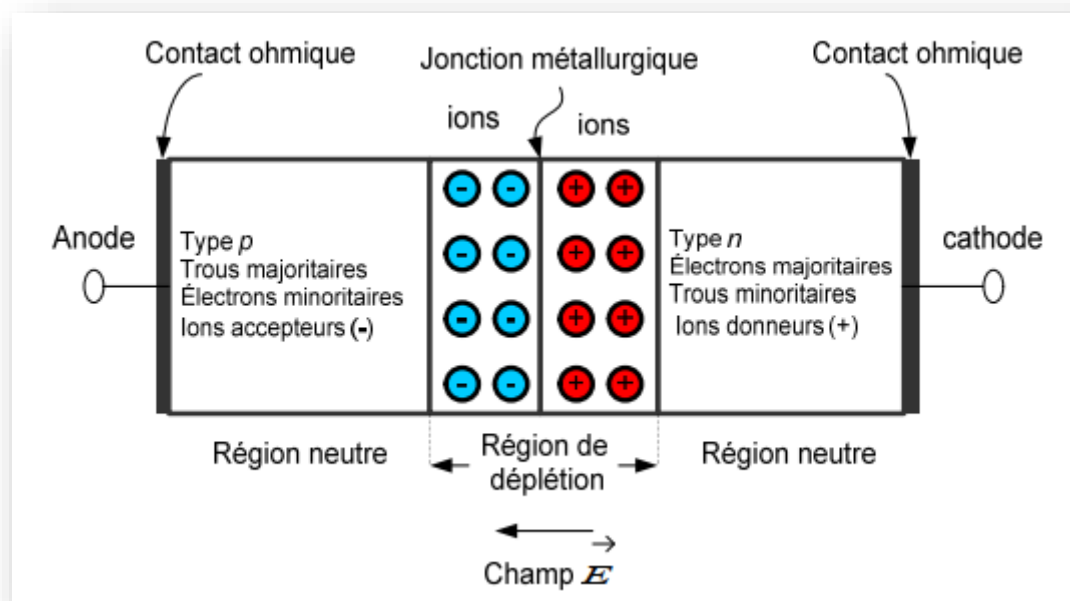


Figure II.1: Representation of a PN junction.

II.3.1. Forward bias of the junction

In forward bias, the junction under a positive voltage V_a which reduces the high voltage barrier that becomes $V_{bi} - V_a$ resulting in decreasing in the width of the depletion region in (Eq II-2) V_{bi} is replaced by $(V_{bi} - V_a)$. Many electrons from the N region and holes from the P region can cross the barrier and then be collected.

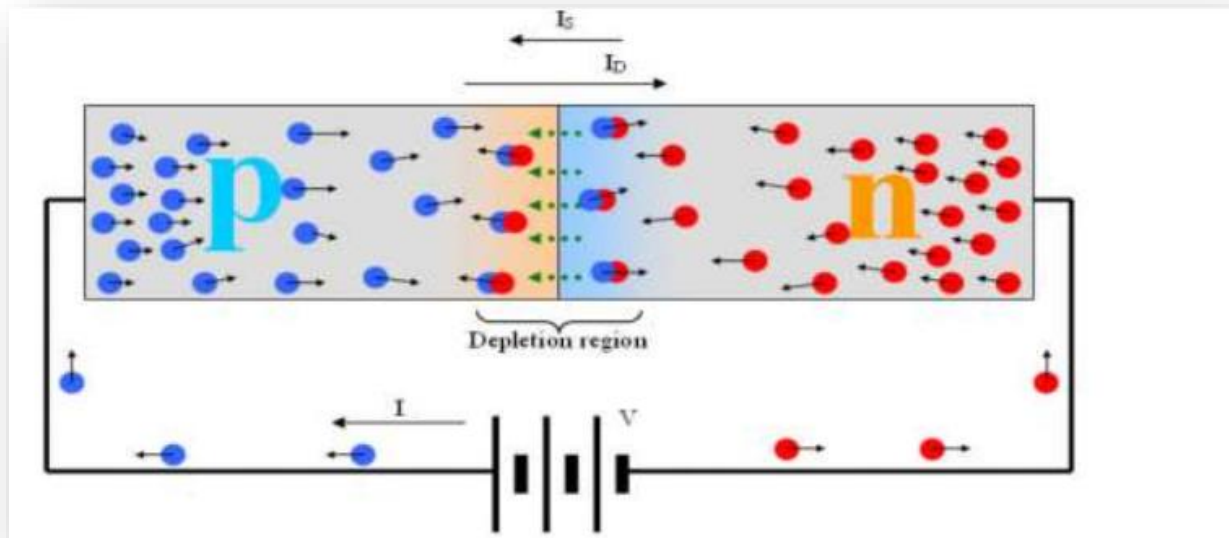


Figure II.2: Forward bias junction.

As the majority carriers or they diffuse and possibly recombine with the majority holes. Also, holes permanently generated in the P region will be available to recombine with electrons crossing the potential barrier.

However, in the forward bias condition, the diffusion current is much larger than the saturation current due to the decrease of the depletion region. The total current is the sum of the saturation current (I_s) and the diffusion current (I_D).

$$I_{\text{total}} = I_s + I_D \approx I_D \quad (\text{II.3})$$

II.3.2.Reverse bias of the junction

Connecting the p-type region to the negative terminal of the voltage supply and the n-type region to the positive terminal corresponds to reverse bias (Figure II.3). If the junction is reverse bias, the height of the potential barrier between the regions P and N is reinforced by the negative applied voltage (V_a) and becomes ($V_{bi}+V_a$). The electric field in the depletion region increases as well as its thickness W (Eq II.4). The majority carriers in the N and P regions do not have the energy to jump this potential barrier. The junction is then crossed by a low saturation current I_s . The (Figure II.3) shows the origin of the reverse saturation current I_s of this junction and the total current is given by (Eq II.5) [25].

$$W = \frac{2\epsilon_s(V_{bi}+V_a)}{e} \left[\frac{N_a+N_d}{N_aN_d} \right]^{1/2} \quad (\text{II.4})$$

$$I_{total} = I_s + I_D \approx I_s \quad (\text{II.5})$$

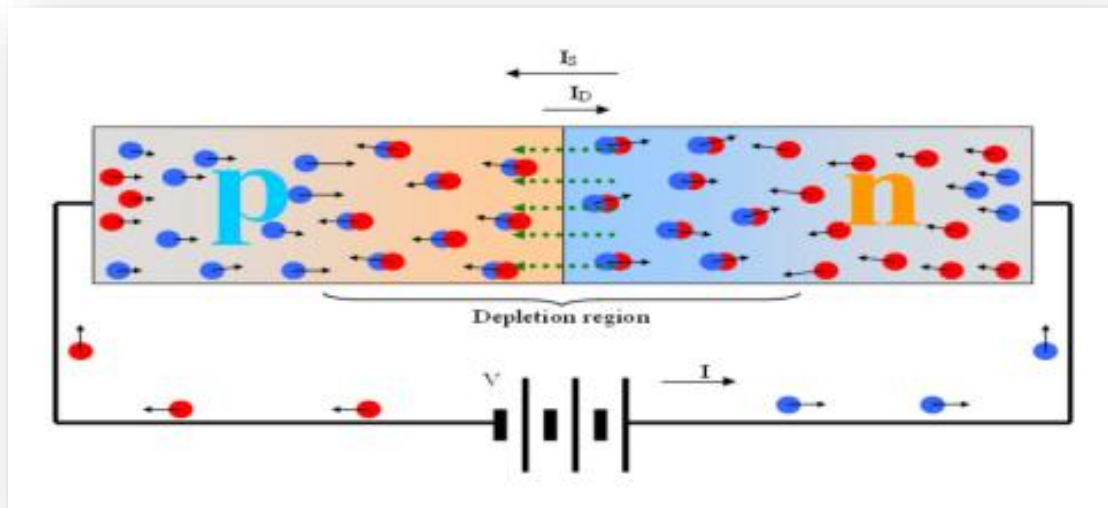


Figure II.3: Reverse bias junction [25].

II.4.Principle of LED operation

Light emitting diode (LED) is a p-n junction diode that is commonly constructed from a direct bandgap semiconductor, such as GaAs, and in which electron hole recombination causes the emission of a photon. Therefore, the energy of the bandgap is roughly equivalent to the energy of the photons that are released. The energy band diagram of an unbiased p-n junction device with a more strongly doped n-side than p-side is shown in Figure (II.4). The band diagram is created to maintain the device uniform Fermi level, which is necessary for equilibrium in the absence of bias. In a p-n⁺ diode, the depletion region mostly encompasses the p-side. The built-in voltage, V_0 , acts as the potential energy (PE) barrier, separating E_c on the n-side from E_c on the p-side. Conduction electrons are more likely to diffuse from the n to the p-side due to the higher concentration of free electrons in the n-side. The electron PE barrier eV_0 , however, prevents this net electron diffusion. Since the depletion zone is the most resistive area of the device, as soon as a forward bias V is applied, this voltage decreases

across the region. The built-in potential V_0 is subsequently decreased to $V_0 - V$, allowing the electrons from the n side to disperse or be injected into the p-side. The spontaneous emission of photons is caused by the hole injection component from the neutral p-side into the n side, which is significantly smaller than the electron injection component. Radiative-recombination mainly takes place in the depletion zone. The active region is another name for this recombination region. The structure of the LED must allow the photons that are released to leave the device without being reabsorbed by the semiconductor [24].

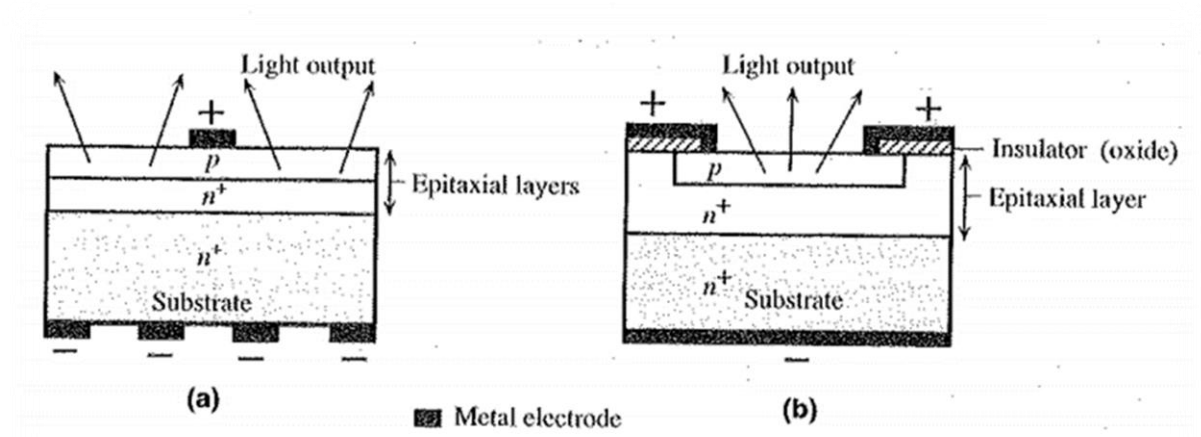


Figure II.4: A schematic illustration of typical planar surface emitting LED devices [24].

II.5. Classification of light emitting diodes

II.5.1. Structure classification

II.5.1.1. Homojunction light emitting diodes

The homo-junctions are made from two blocks of the same nature but different doping to form a PN junction. The recombination of the carriers is predominant in the «p» zone, this phenomenon is explained by the fact that the holes have a much lower mobility than electrons and results in the presence of a greater number of electrons (minority carriers) in the p region than the holes (minority carriers) in the n region. The luminescence is therefore more important on the p side, which is why the LEDs are manufactured with the p region close to the emitting surface. The technology of homo-junction quickly reaches its limits, because by increasing the level of doping to improve the efficiency of injection, we simultaneously

increase the impurities which in turn constitute additional non-radiative recombination centers. In addition, photons generated by the luminescent centre can be reabsorbed.

This radiation trapping increases rapidly with the level of doping. Obtaining diodes producing several hundred lumens requires the implementation of another technology, that of hetero-junction [2].

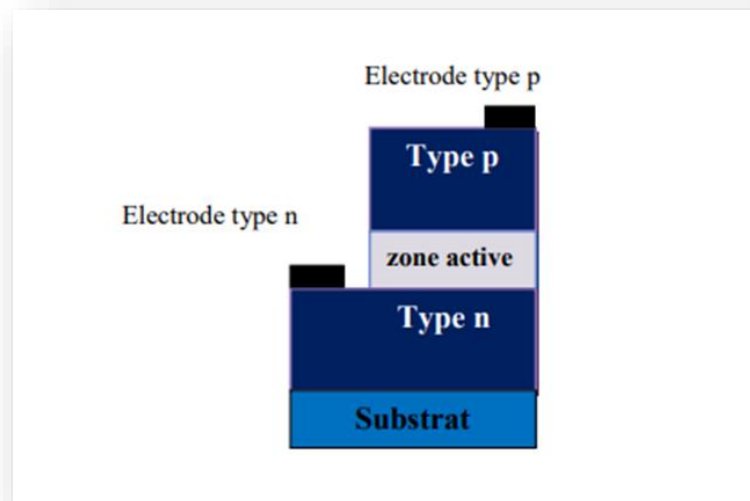


Figure II.5: Structure of a homo-junction LED [2].

II.5.1.2. Heterojunction light emitting diodes

Hetero-junction technology has been developed with the aim of improving injection efficiency i.e. the influence of non-radiative recombinations versus radiative recombinations. A hetero-junction is essentially based on an assembly of two or more semiconductors of different compositions and different degrees of doping (Figure II.6) [26].

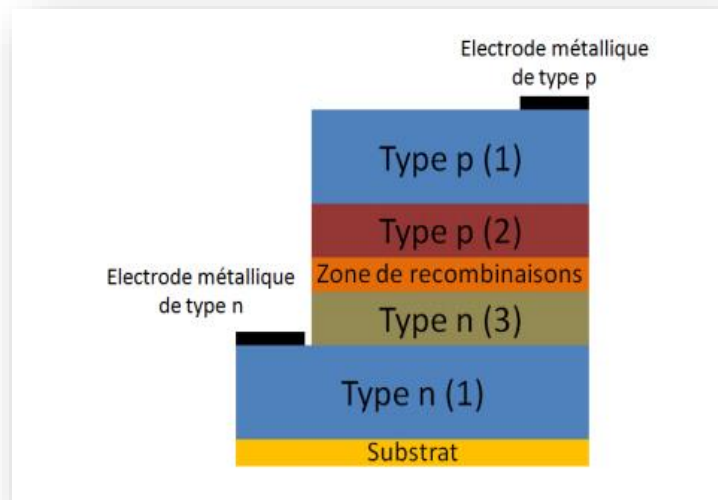


Figure II.6: Schematic diagram of a p-n hetero-junction with three types of semiconductors [26].

II.5.1.3. Quantum well LEDs

A quantum well is obtained by growing a layer of semiconductor material A (typically tens of nanometers) between two layers of another semiconductor material B. The latter has an energy gap greater than that of the material A. The discontinuity between the energy bands in the two materials creates a potential barrier that confines the carriers in the quantum well. The name well and barrier comes from the fact that electrons and holes flow from the barrier material to the well. The well is said to be quantum if its dimensions are small enough (of the order of the nanometer) that the energy levels in it are quantified. The emission wavelength can then be varied between the gap band energy of the well and the barrier by changing the width of the well. When an electrical voltage is applied, the charges are injected into the quantum wells, they recombine and their energy difference is released in the form of a photon (Figure II.7). The quantum well allows having a better radiative efficiency by concentrating the electrons and the holes in a small volume: The recombination electron-holes are then more probable. A single quantum well can be saturated with carriers, so that at high current the number of photons emitted remains constant from a certain threshold. To overcome this problem, structures with multi-quantum wells are manufactured [2].

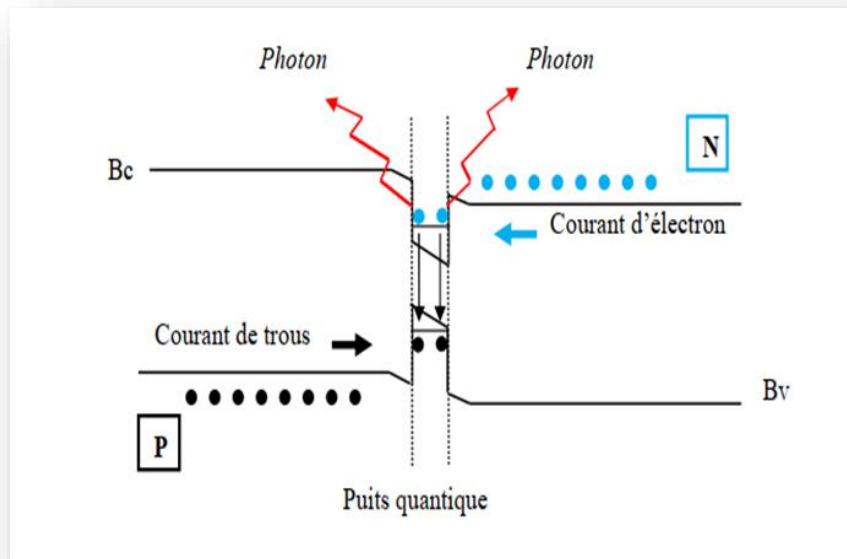


Figure II.7: Quantum well LEDs [2].

II.5.2. Power classification

II.5.2.1. Low-power LED

Figure II.5 shows architecture of a low power LED. Since 1970, low-power LEDs have been present in our daily lives but they are not developed for high power and light flux for lighting applications (Figure II.8) [27, 28].

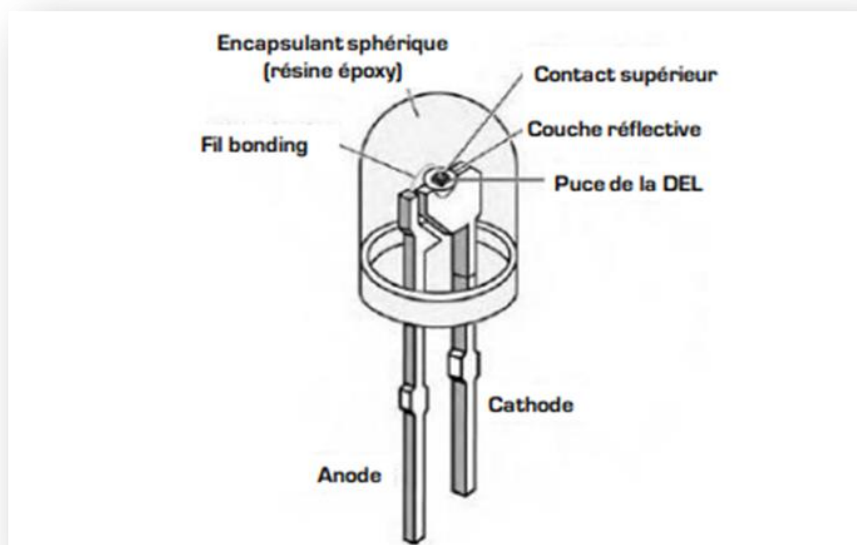


Figure II.8: Architecture of a low power LED [27].

II.5.2.2.High-power LED

The Figure II.9 depicts the architecture of a high power LED. They are frequently used in applications like flash mobile phones and house illumination. The fundamental design is the same as the prior architecture, but the new design includes a compartment called the "thermal pad" whose purpose is to remove heat produced at the chip level. Multiple high-power LED bulbs (HB: high brightness; UHB: extreme high brightness) are utilized for lighting [2].

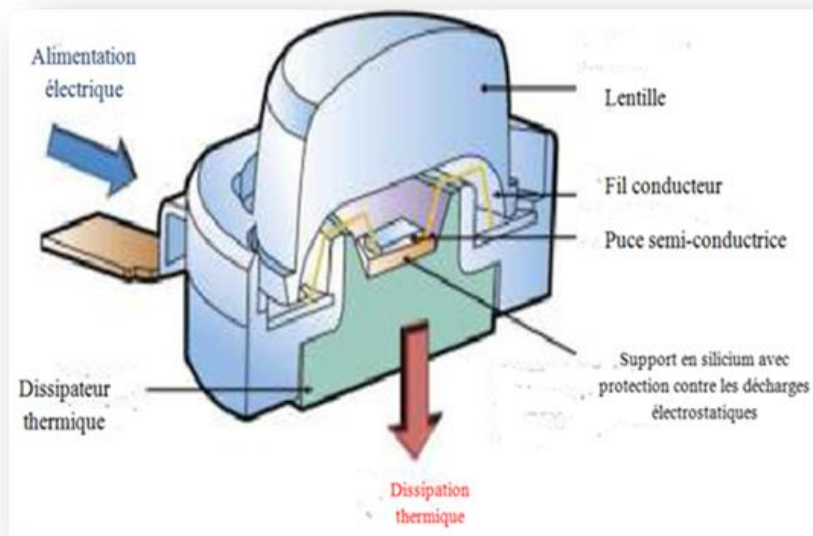


Figure II.9: Architecture of a high power LED [2].

The following table summarizes the characteristics of two families of LEDs:

LED's	Settings
Conventional LEDs (Low power)	<ul style="list-style-type: none"> • Junction surface: 350×350μm • Supply : 30 mA, 3.5v • Power<200W • Flow : 1-3 lumens • Light efficiency (for white diodes) 20 lm/W • Epoxy encapsulation (endôme)
HB-LED high brightness (high power)	<ul style="list-style-type: none"> • Junction surface : 1×1mm² • Supply : 350mA,3.5v • Maximum power : 1W • luminous flux : 5-30 lumens • Light efficiency (for white diodes)>30lm/W • Specific encapsulation (silicone)
UHB-LED very bright	<ul style="list-style-type: none"> • Junction surface : 2×2mm² • Current area density>50A/cm² • Maximum power : 5W • luminous flux>100 lumens • Light efficiency (for white diodes)50lm/W • Specific encapsulation (silicone)

Table II.1: The different families of light emitting diodes [27].

II.5.3.Emission spectrum classification

II.5.3.1.Monochromatic light emitting diodes

Most LEDs produce monochromatic light, and today there are multi-coloured diodes that can produce a range of different colours, consisting of three diodes (RGB LEDs -red, green, and blue LEDs) [28].

II.5.3.2. White light emitting diodes

The production of white LEDs is achieved by using phosphors in order to convert the wavelength of the light emitter to the visible spectrum. To create white light is also dependent on the type of LEDs [8].

II.5.3.3. Infrared light emitting diodes

It is an infrared photoemission (820nm - 1000nm) under reverse bias. Usually, they are fabricated from a material with direct band gap such as Gallium Arsenide [29].

II.6. Properties of light emitting diodes

II.6.1. Optical properties

II.6.1.1. Quantum efficiencies

For each electron injected, the active region of a perfect LED emits one photon. One light quantum-particle (photon) is created for every charge quantum-particle (electron). As a result, the optimum LED active region has a quantum efficiency of one. The definition of the internal quantum efficiency is:

$$\eta_{\text{int}} = \frac{\text{number of photons emitted from active region per second}}{\text{number of electrons injected into LED per second}} = \frac{P_{\text{int}}/(h\nu)}{I/e} \quad (\text{II.4})$$

Where:

P_{int} : is the optical power emitted from the active region .

I : is the injection current.

The LED should allow photons released by the active region to escape. In a perfect LED, the active region emits all of its photons into empty space. A LED of this type has unity extraction efficiency. However, not all of the power emitted from the active region of a real LED is sent into space. This results from a number of loss processes. For instance, if the LED substrate is absorbent at the emission wavelength, light from the active region may be not present there. The definition of the extraction quantum efficiency is:

$$\eta_{\text{extraction}} = \frac{\text{number of photons emitted into free space per second}}{\text{number of photons emitted from active region per second}} = \frac{P/(h\nu)}{P_{\text{int}}/(h\nu)} \quad (\text{II.5})$$

Where:

P: is the optical power emitted into free space.

The external quantum efficiency is defined as:

$$\eta_{\text{power}} = \frac{P}{P_{\text{elec}}} \quad (\text{II.6})$$

Where:

P_{elec} : is the electrical power provided to the LED equals I.V.

II.6.1.2.Emission spectra

The spectrum of an LED is often expressed by a single wavelength. LEDs are moderately narrowband emitters with an approximately Gaussian spectral shape. The most common spectrum-based description is the peak wavelength, λ_p , which is the wavelength of the peak of the spectral density curve. Less common is the center wavelength, $\lambda_{0.5m}$, which is the wavelength halfway between the two points with a spectral density of 50% of the peak. For a symmetrical spectrum, the peak and center wavelengths are identical. However, many LEDs have slightly asymmetrical spectra. Least common is the centroid wavelength, λ_c , which is the mean wavelength. The peak, center, and centroid wavelengths are all derived from a plot of $S_\lambda(\lambda)$ versus λ [31].

II.6.1.3.Optical power

The total optical power radiated by the LED is expressed in W/cm^2 and can be calculated using the following formula:

$$P = \int_A \int_\lambda I(\lambda) d\lambda dA \quad (\text{II.7})$$

Where:

$I(\lambda)$: is the spectral light intensity (measured in W per nm per cm^2).

A: is the surface area of the sphere.

The distance from the LED affect the intensity and the integration is carried out over the entire surface area [32].

II.6.1.4. Luminous efficiency of light emitting diodes

The effectiveness of converting optical power to luminous flux is known as the luminous efficacy of optical radiation, also known as the luminosity function, and is expressed in lumens per watt of optical power. It is given by the following formula:

$$\text{Luminous efficacy} = \frac{\phi_{\text{lum}}}{P} = \left[683 \frac{\text{lm}}{\text{W}} \int_{\lambda} V(\lambda) P(\lambda) d\lambda \right] / \left[\int_{\lambda} P(\lambda) d\lambda \right] \quad (\text{II.8})$$

The luminous efficacy for absolutely monochromatic light sources ($\Delta\lambda \rightarrow 0$) is equal to the eye sensitivity function $V(\lambda)$ times 683 lm/W. However, the luminous efficacy of multicolour light sources, and particularly white light sources, must be determined by integration over all wavelengths. The luminous flux of a light source is divided by the electrical input power to determine its luminous efficiency, which is also expressed in units of lm/W.

$$\text{Luminous efficiency} = \phi_{\text{lum}} / (I V) \quad (\text{II.9})$$

where $(I V)$ represents the device electrical input power. Table II.2 lists the luminous efficiency of common light sources [30].

Light source		Luminous efficiency
Edison's first light bulb (with C filament)	(a)	1.4 lm/W
Tungsten filament light bulbs	(a)	15-20 lm/W
Quartz halogen light bulbs	(a)	20-25 lm/W
Fluorescent light tubes and compact bulbs	(b)	50-80 lm/W
Mercury vapor light bulbs	(c)	50-60 lm/W
Metal halide light bulbs	(c)	80-125 lm/W
High-pressure sodium vapor light bulbs	(c)	100-140 lm/W

Table II.2: Luminous efficiencies of different light sources [30].

II.6.2. Electrical properties

A light emitting diode is a p-n junction. The expression of current as a function of the applied voltage in a diode of width A is given by:

$$I = eA \left[\sqrt{\frac{D_p}{\tau_p}} N_A + \sqrt{\frac{D_n}{\tau_n}} N_D \right] e^{\frac{e(V-V_D)}{kBT}} \quad (\text{II.10})$$

Where $D_{n,p}$ are the diffusion constants of electron-holes and $\tau_{n,p}$ are the life times of these minority carriers. N_D and N_A are the donor and acceptor concentrations respectively. The exponential term shows a rapid increase in current when the V_D voltage arrive at the threshold voltage. The V_D value depends essentially on the energy of the forbidden band of the semiconductor forming the diode. In its normal operation, a LED is used in forward bias condition, which is when the current circulates from the anode to the cathode.

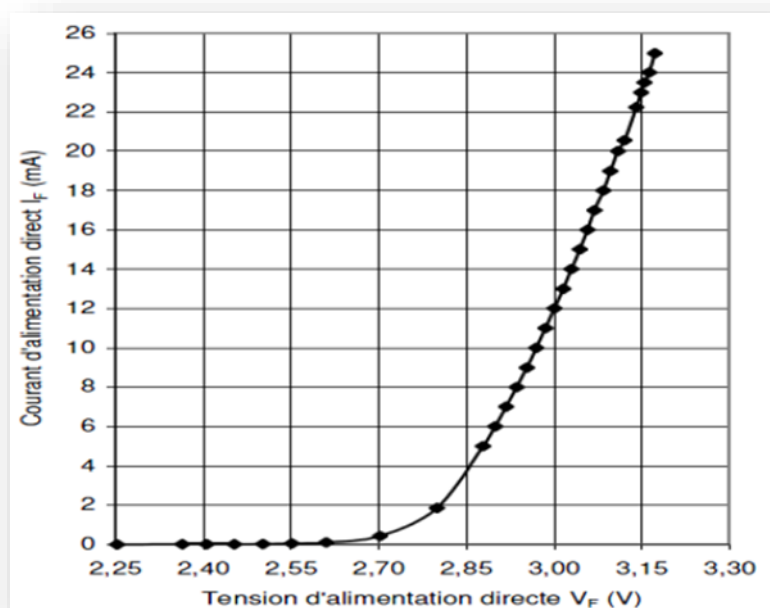


Figure II.10: LED voltage current characteristic [30].

II.7.Applications of LEDs

The use of LEDs has advanced significantly with technological development. They can be used specifically:

- In remote controls, to transmit data.
- In the manufacture of large LED screens.
- In the health sector and in biology,
- In telemetry (ultrasonic transmitter and receiver)

Table II.3 shows some of the applications of the various families of LEDs.

LED's	Applications
Conventional LEDs (Low power)	Mobile applications and signalling
HB-LED high brightness (high power)	Backlight, automotive, lighting
UHB-LED very bright	General lighting

Table II.3: Some of the applications of the various families of LEDs [27].

II.8.Advantages and disadvantages of light emitting diodes

II.8.1.Advantages

Compared to ordinary bulbs, LEDs have enough advantages:

- In the manufacture of electronic circuits, they can be assembled without any difficulty.
- Low consumption.
- Much longer life time.
- Very low voltage operation.
- When switched on, they switch on and off in a very short time (transmission of signals).
- They are robust and resistant (shocks, mechanical vibration).

- Their relatively small size makes it possible to achieve light sources with good efficiency by assembling several LEDs.

II.8.2.Disadvantages

Despite all the advantages of LEDs, they have some disadvantages:

- As the LED is composed of semiconductors, the more it heats up its direct junction voltage decreases; this effect affects its light output which degrades.
- Non-uniform distribution of spectral energy of white LEDs (between 380 and 780 nm) [27].

Chapter III

SILVACO-ATLAS and simulation results

III.1.Introduction

Simulation is a powerful technique for mathematically simulating how devices and systems operate. It is frequently employed when analytical methods are insufficient to accurately depict the system under study. For instance, in some circumstances, the objective function is nonlinear, making it impossible to express some of the constraints using a set of linear equations. In other instances, the results are significantly impacted by the analytical method simplifications used. The creation and forecasting of the characteristics of contemporary technologies likewise heavily rely on simulation. Modern technologies, like integrated circuits, have relatively high costs due to trial production and circuit redesign, which can be significantly reduced via simulation. In a simulation, a semiconductor device is represented by a structure whose electrical and physical characteristics are discretized onto a mesh of nodes that contain details on the different types of materials used, doping profiles in certain areas, and boundary conditions. To describe the physical behaviors of the device, a large collection of physical models is also provided. Through the use of iterative numerical techniques, a device simulator determines the output characteristics by solving a group of partial differential equations [32].

III.2.Presentation of the SILVACO program package

The ATLAS SILVACO (Atlas Silicon Valley Company) environment makes it possible to conceptualize and predict the performance of semiconductor device. This tool is used to simulate semiconductor device designs before they are manufactured. Many research projects have been made possible by ATLAS SILVACO. New physical models are included in ATLAS-SILVACO that make advantage of effective numerical algorithms, innovative meshing techniques, optimization of linear solutions, to provide simulations that are remarkably accurate. This kind of simulators' main benefit is that it allows users to perceive physically real-world occurrences that are otherwise difficult to observe. For electrical simulation of components like diodes, MOSFETs, MESFETs, bipolar transistors, ATLAS-SILVACO modules can be used [33].

III.2.1.ATLAS

The ATLAS simulation tool is a component modeling simulator electronics; it is able to predict the electrical characteristics of most semiconductor components in DC, AC, and transient or frequency conditions. In addition to "external" electrical behavior, it provides information on the internal distribution of variables such as carrier concentrations, current lines, electrical field or potential and important data for process design and optimization. This is achieved by digitally solving the Poisson equation and the two-dimensional electron and hole continuity equations into a finite number of points forming the mesh of the user-defined structure. This simulator is composed of two parts:

- A part of digital processing (integration method, discretization...).
- Some of the most recent physical models of semiconductor components: Models of recombination, impact ionization, temperature-dependent mobility, statistics of Fermi-Dirac and Boltzmann in particular.

The diagram in Figure IV.4 shows the different types of information that circulate in and out of ATLAS during the simulation. The first type of file is the "Runtime Output" file. The second type of file is the "log" file which stores all the voltage and current values from the analysis of the simulated device (this is the electrical behavior file).

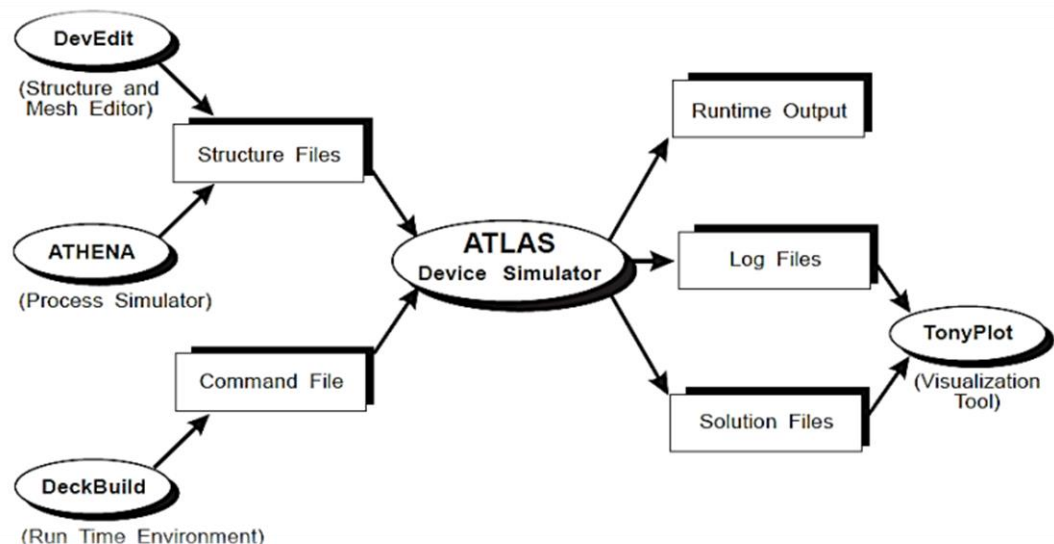


Figure III.1: Input and output information types of the ATLAS simulator [34].

The third output file is the «Solution file», this file stores the data concerning the values of the solution variables at a given point in the device (this is the physical file, it contains the

structure in a particular state). The last two files are processed by the visualization tool TonyPlot [34].

III.2.1.1. Deckbuild

Deckbuild is a powerful runtime tool that allows the user to seamlessly move from process simulation to device simulation to SPICE model extraction. It is easy to use the runtime environment to run basic simulators such as Atlas. Deckbuild helps create input files to Atlas. Several windows provide menu-based or text-based input bridges for the input information. It also includes a large number of examples for all types of technologies. Other simulation tools such as Tonyplot, Devedit and Maskview can also be invoked from Deckbuild. Deckbuild optimizers help optimize targets such as structural dimensions and device parameters after complicated electrical tests and intermediate outputs. An example is shown in Figure (III.2) [35].

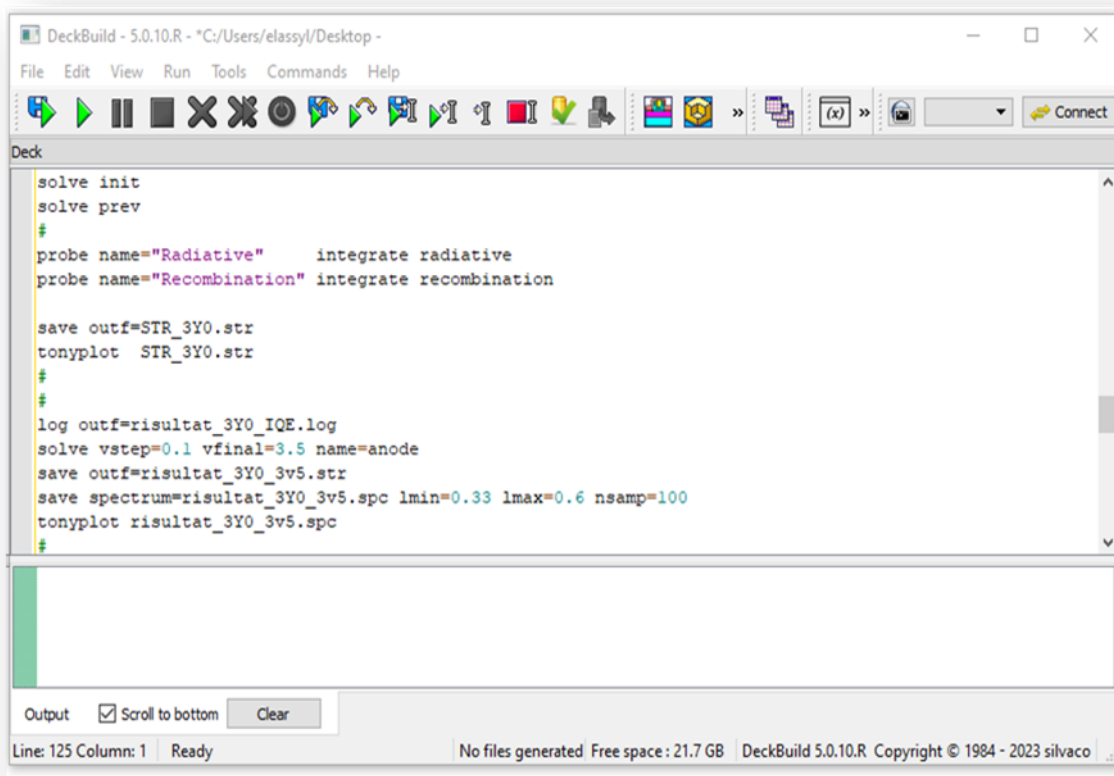


Figure III.2: Deckbuild interface.

III.2.1.2. Tonyplot

Tonyplot is a tool that allows visualizing simulation results such as the structure of the electronic component in 2D or 3D, the band diagram, the mesh and electrical characteristics [27].

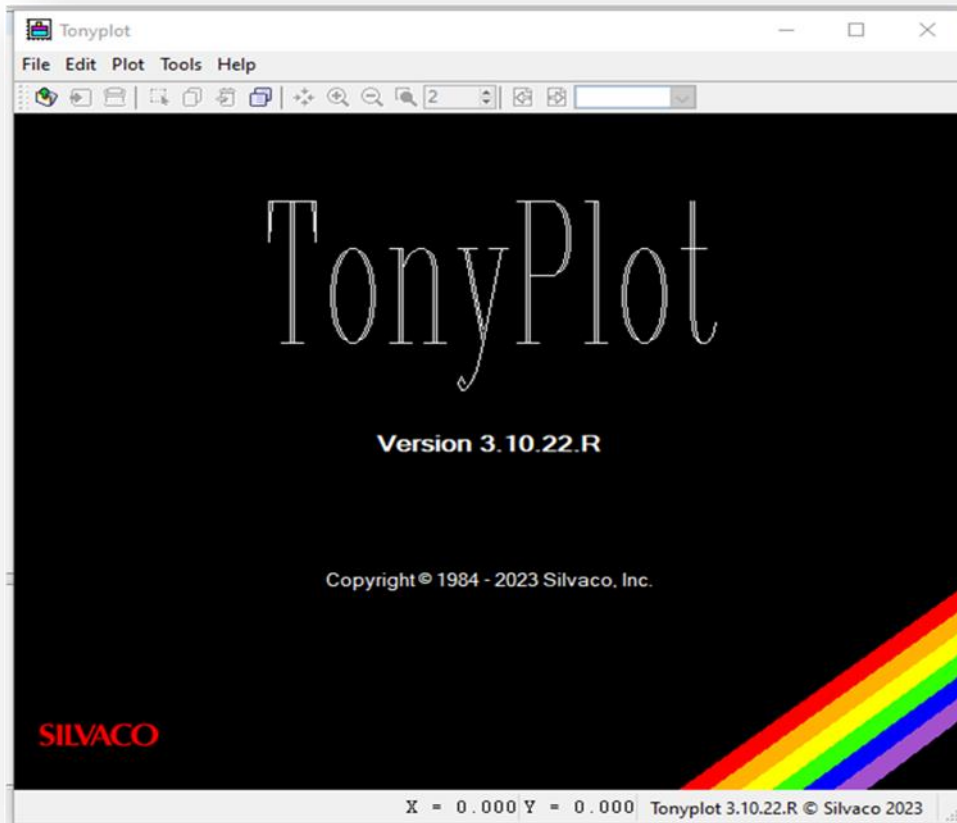


Figure III.3: Tonyplot window.

III.2.2. Basic semiconductor equations in ATLAS-SILVACO

A mathematical model that can be applied to every semiconductor device has been developed as a consequence of years of research into device physics. The electrostatic potential and the carrier densities are connected by a series of basic equations in this model within a simulation area. These equations were derived from Maxwell's laws and include

Poisson's Equation and the continuity equations, which may be calculated in any general-purpose device simulator.

Poisson's Equation relates the electrostatic potential to the space charge density:

$$\text{div} (\varepsilon \nabla V) = q (n - p - N_d^+ + N_a^-) \quad (\text{III.1})$$

Where:

ε : is the dielectric constant.

V : The potential.

q : is the elemental charge of electrons. N_d^+ and N_a^- : are the concentrations of the ionized donor and acceptor dopants.

n and p : are the densities of the free carriers.

The continuity equations for electrons and holes are defined by equations:

$$\frac{\partial n}{\partial t} = G_n - R_n + \frac{1}{q} \text{div} \vec{j}_n \quad (\text{III.2})$$

$$\frac{\partial p}{\partial t} = G_p - R_p + \frac{1}{q} \text{div} \vec{j}_p \quad (\text{III.3})$$

where :

n and p : are the electron and hole concentration,

j_n and j_p are the electron and hole current densities.

G_n and G_p : are the generation rates for electrons and holes.

R_n and R_p : are the recombination rates for electrons and holes.

q : is the magnitude of the charge on an electron [36].

III.2.3.Syntax of a program in ATLAS

III.2.3.1.Mesh

This command produces a mesh or reads a mesh that has been defined previously. The mesh element used is the triangle [37].

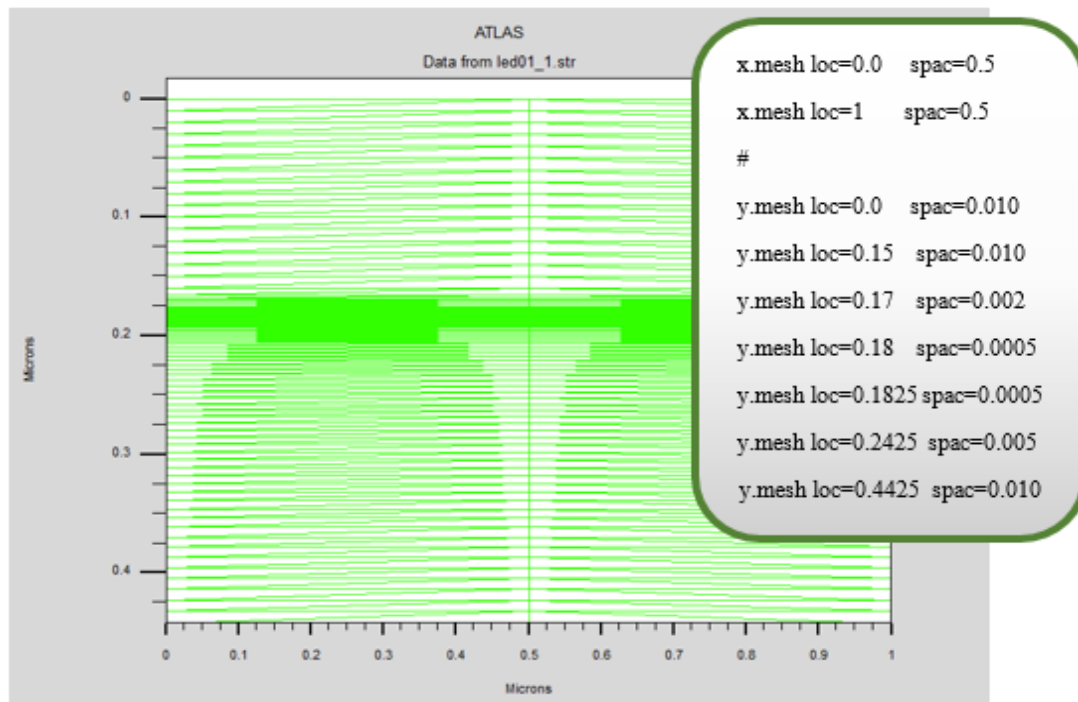


Figure III.4: Mesh definition with Atlas.

III.2.3.2.Region

After defining the mesh, it is necessary to define the regions whose format for defining the regions is as follows:

REGION number = < integer ><type_material> / <parameter_position>.

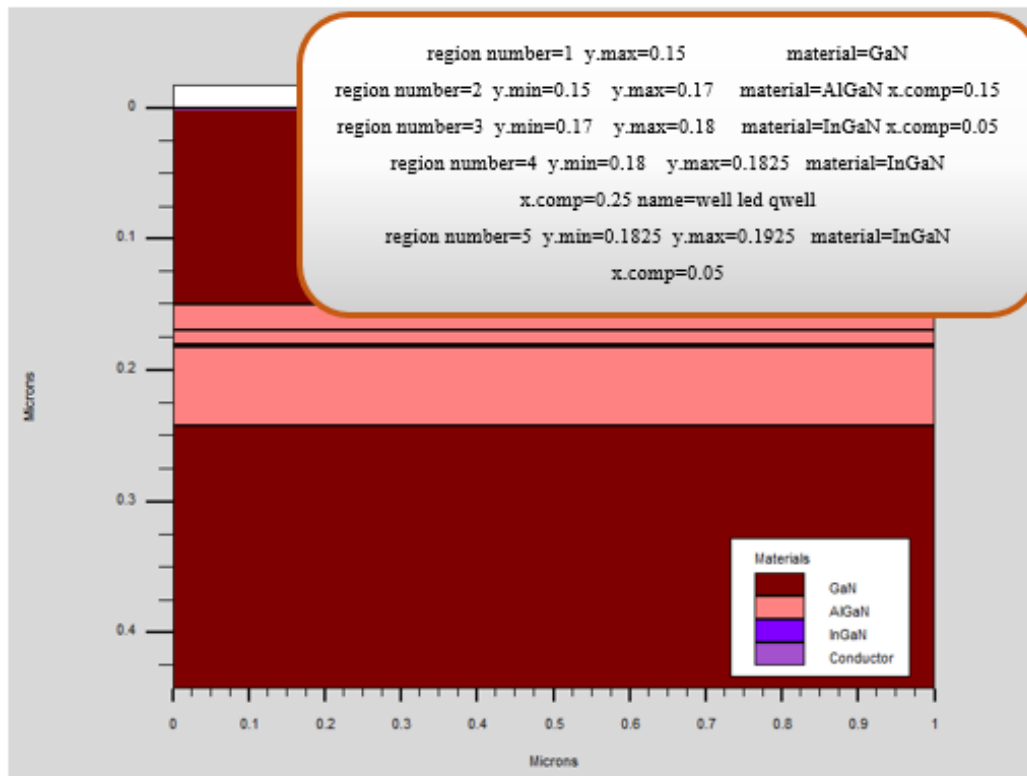


Figure III.5: Regions with defined materials.

III.2.3.3.Electrode

Atlas has a maximum of 50 electrodes that can be defined. The electrode definition format is as follows:

ELECTRODE NAME = < electrode name ><parameter_position>.

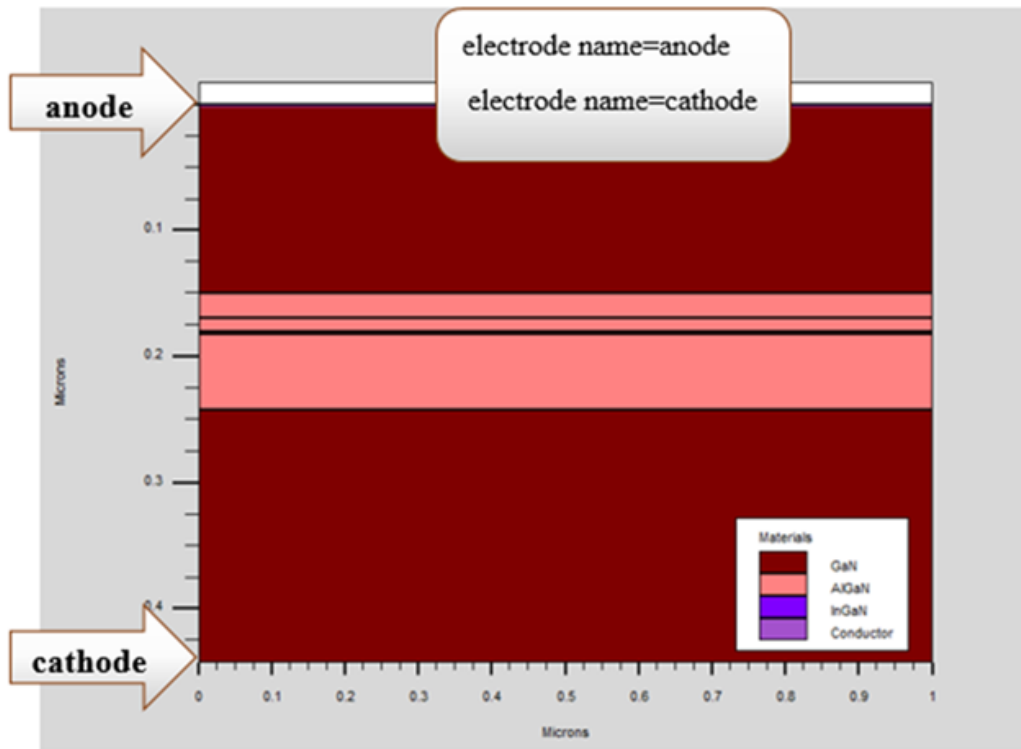


Figure III.6: Electrode definition.

III.2.3.4.Doping

The last aspect of the structure specification that needs to be defined is doping. The format of the doping report in Atlas is as follows:

DOPING <type_distribution><type_dopant> / <parameter_position> [38].

For example:

doping region=1 uniform p.type conc=1e19

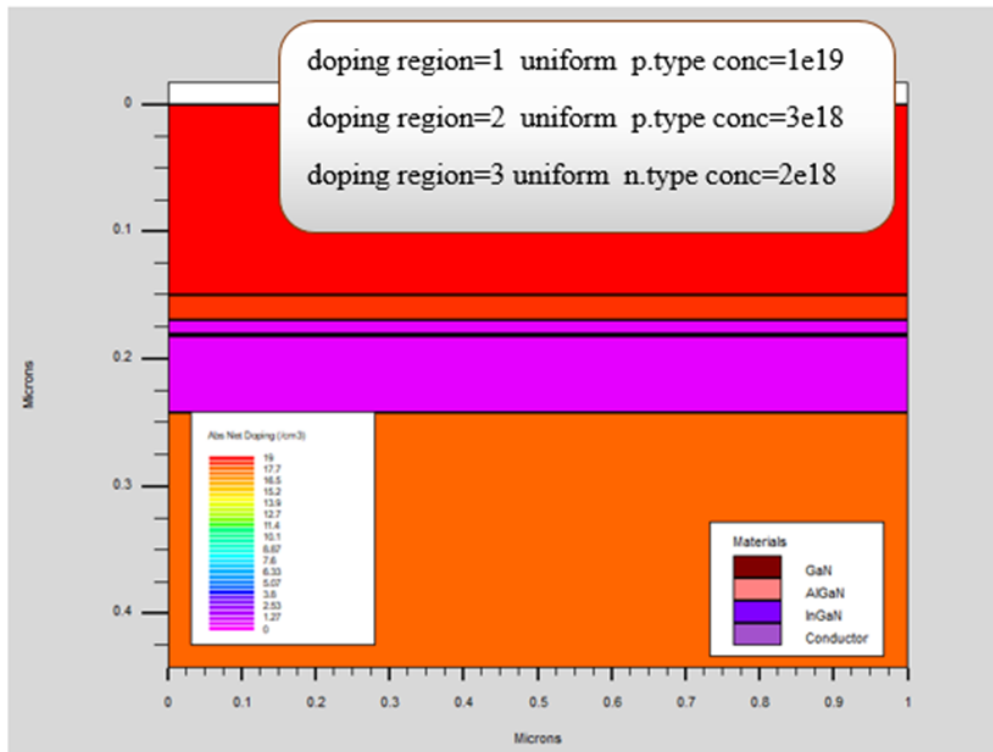


Figure III.7: Distribution of doping in the regions.

III.2.4.Specification of material parameters and physical models

After defining the structure, it is necessary to specify the models of the materials, it consists of four parts: material, models, contact and interface.

III.2.4.1.Materials

The atlas declaration format for materials is as follows:

MATERIAL < identification >< material parameter >

Several parameters can be identified for the material of a given region, for example:

material material=GaN taun0=2e-7 taup0=2e-7 copt=1.1e-8 augn=1e-31 augp=1e-31

III.2.4.2.Models

Physical models fall into five categories: mobility, recombination, transporter statistics, ionization impact, and tunnel effect. The syntax of the template declaration and as follows:

MODEL< general parameters > / < model parameters >

Example:

models k.p fermi incomplete srh auger optr print

models name=well k.p chuang spontaneous lorentz

models polarization calc.strain polar.scale=0.15

model auger srh fermi print temperature=300

The choice of model depends on the materials chosen for the simulation.

III.2.5.Selection of the numerical method

After specifying the material models, the choice of numerical method must be made.

The only declaration that applies to the selection of the numerical method is the method declaration. A variety of numerical methods exist to calculate solutions [39]:

- The decoupled method (GUMMEL).
- The coupled method (NEWTON).
- BLOCK.

III.2.6.Solution Specification

After completing the selection of the numerical method, the next step is the specification of the solution. The solution specification is broken down into these declarations Log, Solve, Load, and Save.

III.2.6.1.Log

Log saves all final characteristics in a file. DC, transient, or AC data is generated by the Solve declaration after a log declaration has been saved.

The following example shows an example of the Log declaration.

```
log outf=led01.log
```

In this example, the log declaration saves the current-voltage data in file led01.log.

III.2.6.2.Solve

The Solve statement follows the Log statement, Solve performs a solution for one or more polarization points. This declaration is in the following format:

```
Solve <bias_points>
```

For example:

```
solve name=anode vstep=0.05 vfinal=3.5
```

III.2.6.3.Save

The Save instruction introduces all the information assigned to a node in an output file (output file).The instructions for save are as follows:

```
Save outf=led01_3p5.str
```

III.2.7.Analyse of results

Results using extract and tonyplot parameters are permitted in Atlas.

III.2.7.1.EXTRACT

Once the solution is found for a semiconductor device problem, the information can be displayed graphically by TonyPlot. In addition, the device can be extracted by the Extract declaration [35].

```
Example: Extract name="IQE" curve(i."anode",probe."Radiative"/probe."Recombination")  
outfile="led01_IQE.dat"
```

III.2.7.2.TONYPLOT

Using TONYPLOT, it is possible to plot data on the device structure, doping profiles, band characteristics, electron and hole concentrations, and electric fields. [36]

```
Example: tonyplot led01_1.str
```

III.3.Simulation results

III.3.1.Representation of the simulated structure

Optical gain and spontaneous recombination models implemented in ATLAS are used to account the effects of quantum well confinement of carriers and strain effects in Multiple Quantum Wells (MQW). To enable these models, we have to use the MQW statement. The MQW statement has parameters describing the locations and compositions of the wells, the effects of strain on the band edges, parameters relating to the gain and recombination models, and parameters relating to how the models interact with other electrical and optical simulations models.

Figure (III.8) shows the studied structure of multiple quantum well LED. The structure consists of fourteen regions. First one, a 200 nm n-type GaN with a doping concentration of $2 \times 10^{18} \text{ cm}^{-3}$. Followed by six regions of undoped $\text{Al}_{0.05}\text{Ga}_{0.95}\text{N}$ which represents the quantum barriers with 10 nm thickness. Then, five regions of undoped $\text{In}_{0.15}\text{Ga}_{0.85}\text{N}$ which represents the quantum wells with 2.5 nm thickness. A 20nm p- $\text{Al}_{0.25}\text{Ga}_{0.75}\text{N}$ with a doping concentration of $3 \times 10^{18} \text{ cm}^{-3}$ and 150nm p-GaN of doping concentration of $1 \times 10^{19} \text{ cm}^{-3}$, are deposited on quantum wells, respectively. In addition, tow electrodes, cathode and anode, are connected on bottom and top, respectively.

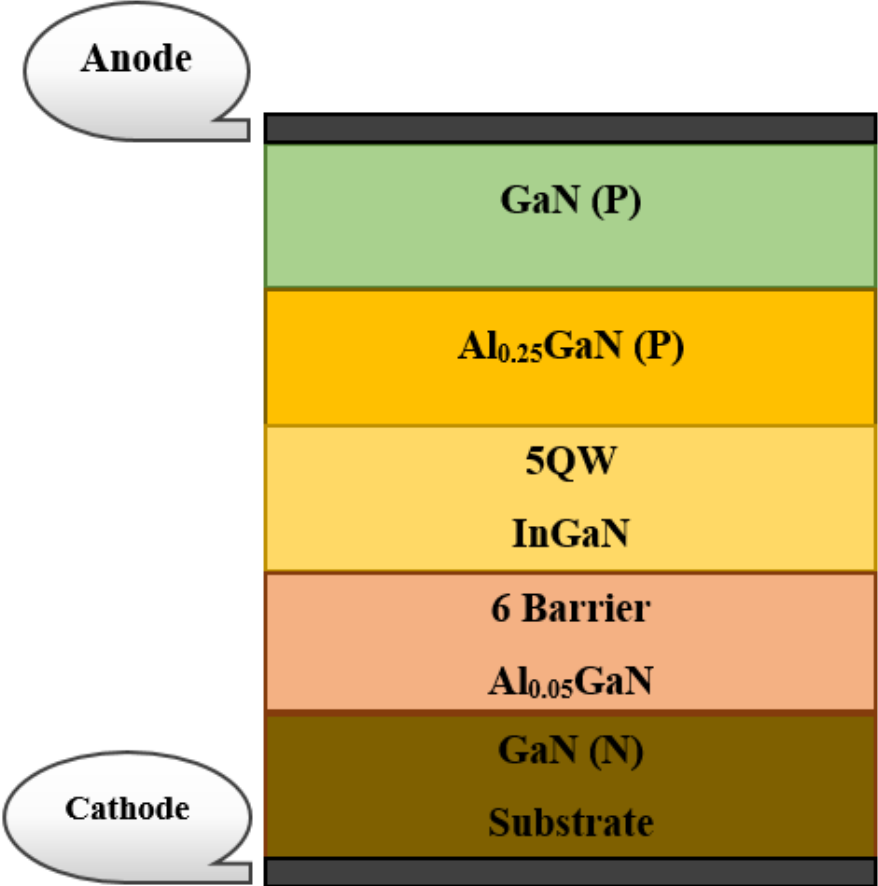


Figure III.8: Diagram of the simulated structure.

Figure (III.9) represents the structure design through the Silvaco Atlas simulator.

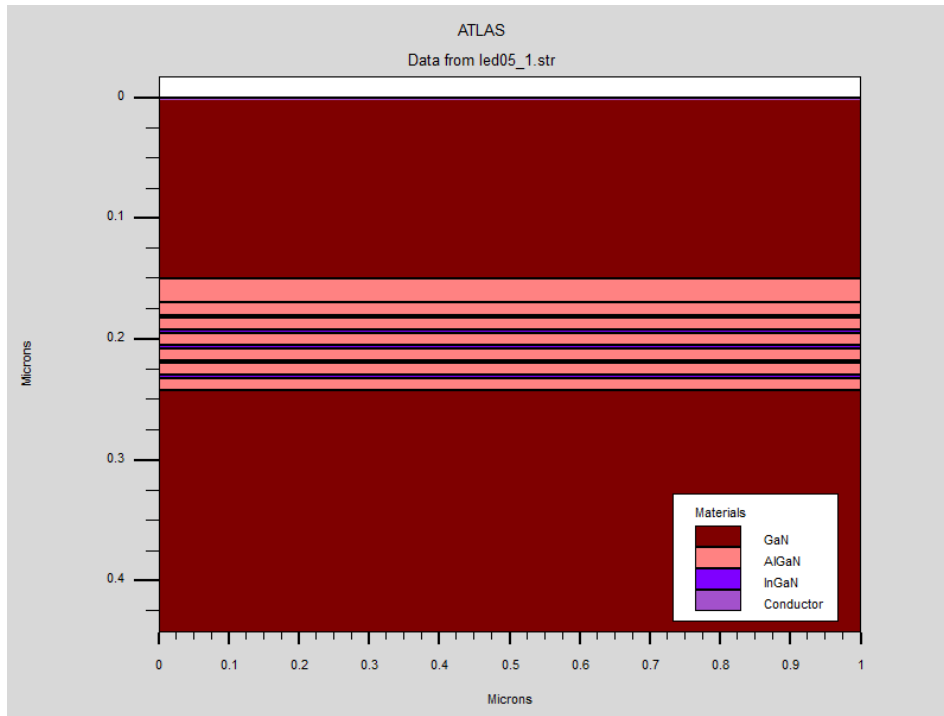


Figure III.9: Structure of the multiple quantum well (5QWs) LED.

III.3.2.Simulation parameters of the LED

In order to simulate a device, it is necessary to determine the parameters of the materials used in the conception of the device, such as gap energy (eV), electron and hole mobility (cm^2/Vs), doping (cm^{-3}) and thickness (nm) and type of materials (AlGa_N, GaN, InGa_N). These parameters are recorded in the following table (III.1).

Parameter Materials	Type p or n	Thickness [nm]	Doping [cm^{-3}]	Hole mobility [$\text{cm}^2/\text{V-s}$]	Electron mobility [$\text{cm}^2/\text{V-s}$]	Band gap (at 300 K) E_g (eV)
GaN	p	150	$1\text{e}19$	10	400	3.42
$\text{Al}_{0.25}\text{Ga}_{0.75}\text{N}$	p	20	$3\text{e}18$	5	250	3.62
$\text{In}_{0.15}\text{Ga}_{0.85}\text{N}$ (5QWs)	-	2.5	-	10	200	2.6
$\text{Al}_{0.05}\text{Ga}_{0.95}\text{N}$ (6 Barriers)		10		5	250	3.62
GaN (substrate)	n	200	$2\text{e}18$	10	400	3.42

Table III.1: Parameters of materials used in simulations.

The active region consists of Multi-Quantum Well (MQW) structure in order to obtain an optimum carrier overflow and efficiency. Hence there is a need for the optimization of multiple quantum well structure. The structure was optimized by changing the number of quantum wells and the applied voltage. The optical and electrical properties of InGaN/GaN MQW LED are investigated numerically with Silvaco ATLAS-TCAD simulation program by extracting the integrated radiative recombination rate and total integrated recombination rate. Both optical and electrical characteristics of the device like Internal Quantum Efficiency (IQE) and turn-on voltage are examined carefully to obtain optimum results.

III.3.3.Current-Voltage characteristic

By changing the quantum wells from two to five under room temperature 300K and varying the bias voltage from 0V to 6V, figure (III.10) represents the current-voltage (I-V) characteristic obtained for the simulated LED diode.

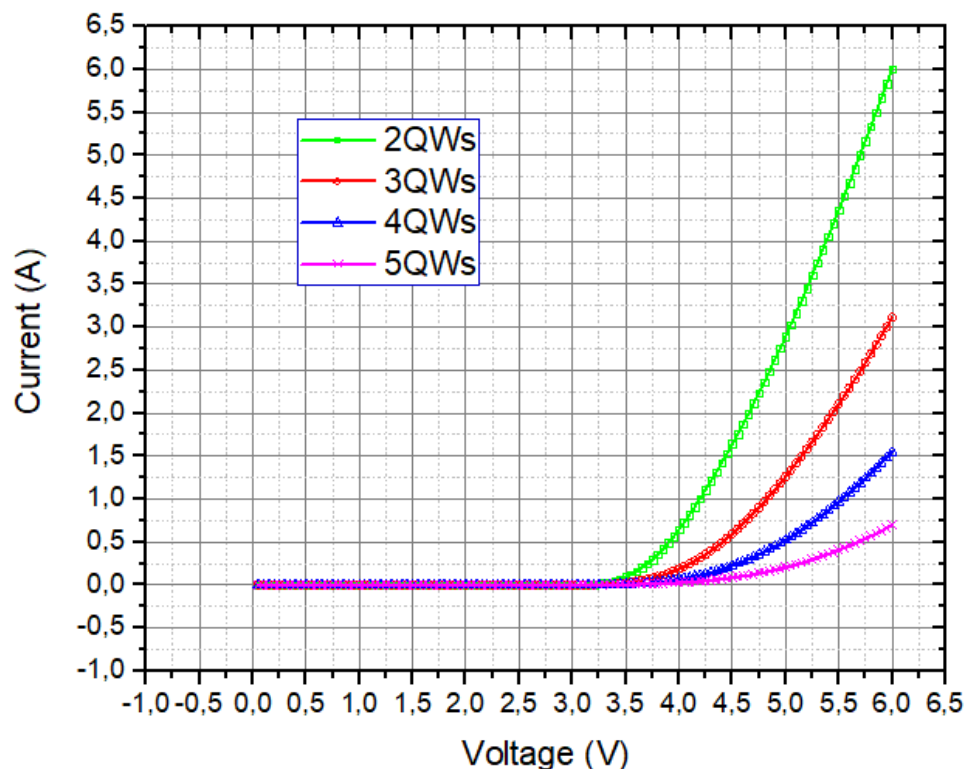


Figure III.10: I-V characteristics of MQW LED for different number of quantum well.

As we can see, all the curves have the same appearance as a p-n junction. The turn on voltage for 2QWs, 3QWs, 4QWs and 5QWs LED at the injection current of 0.5 A is 3.62 V, 4.00V, 4.25V and 4.37 V respectively. Normally, it is believed that forward voltage should increase as the number of MQW increases, which is due to the increase of series resistances induced by the increase of QWs number.

III.3.4.Spectral power

The spectral power of the simulated structure for different quantum well LED is shown in the figure (III.11).

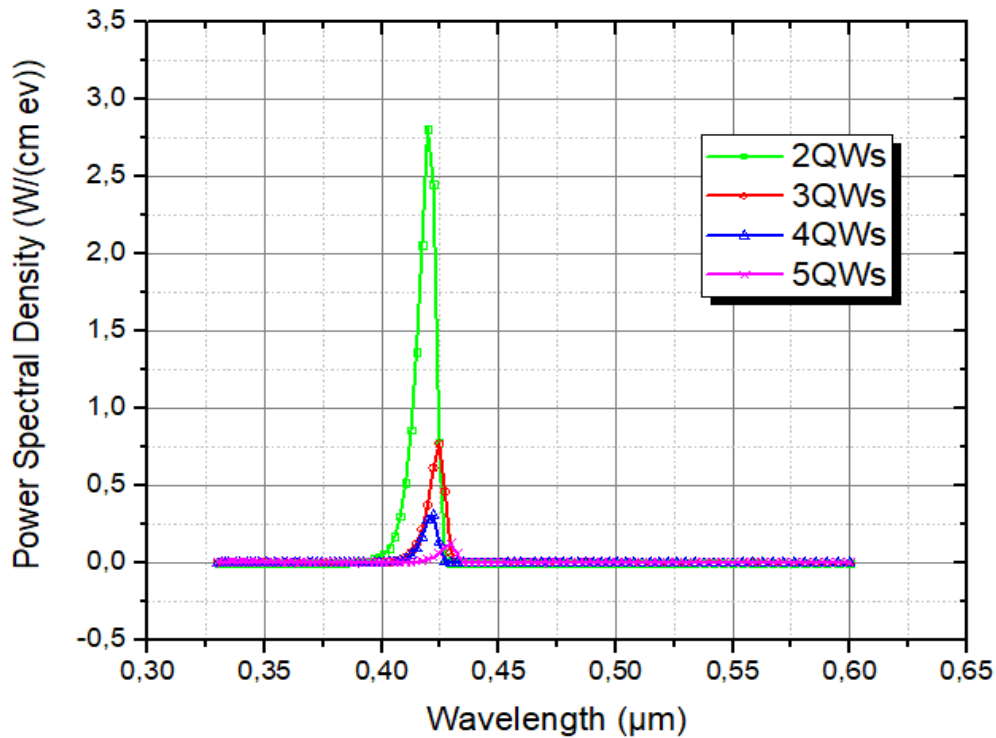


Figure III.11: Power spectral density for different quantum well LED.

This curve shows maximum light emission at a different quantum well. The wavelength value of the peak emission spectrum indicates which part of radiation is emitted.

Figure (III.11) shows the peak wavelengths emitted for different quantum wells, namely:

- 2QWs, the maximum emission occurs at the 0.422 μ m wavelength.
- 3QWs, the maximum emission occurs at the 0.429 μ m wavelength.
- 4QWs, the maximum emission occurs at the 0.425 μ m wavelength.
- 5QWs, the maximum emission occurs at the 0.43 μ m wavelength.

As can be seen, all the spectra of LED diode emissions are relatively narrow. Comparing different spectrums shows that the difference between the intensity of LED emission spectrums is caused by the different number of quantum wells. We also note from figure (III.11) that there is a little shift in the position of the peak as the number of the quantum well increases and the wider spectrum is attributed to the 2QWs LED.

III.3.5.Luminous Power

The variation of luminous power versus the current is shown in figure (III.12). It is clear that as the current increase, more the luminous is increased. Some values are giving below at fixed current of 3.5A.

- 2QW, its maximum value of 5.53W at 3.5A.
- 3QW, its maximum value of 3.82W at 3.5A.
- 4QW, its maximum value of 1.95W at 3.5A.
- 5QW, its maximum value of 0.52W at 3.5A.

The value of luminous power in case of 2 quantum wells is greater than in cases of 3, 4 and 5 quantum wells.

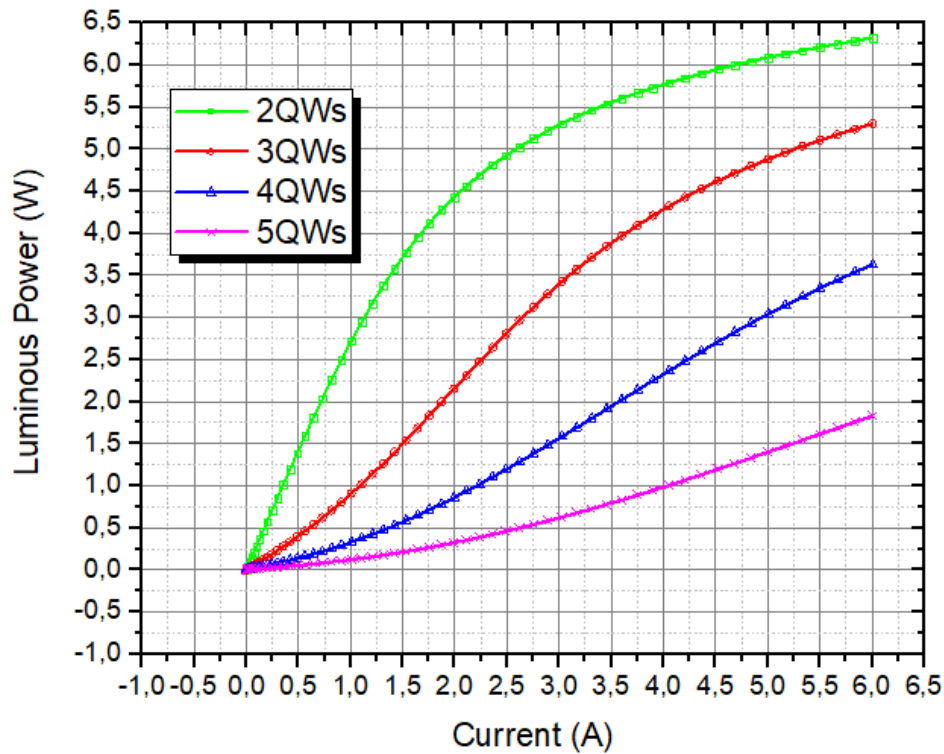


Figure III.12: Luminous power for different quantum well.

III.3.6.Spectral power of 2QWs at different voltages

The spectral power of 2QWs for different bias voltage 3.5V, 4.0V and 5.0V is shown in the figure (III.13). it is observed that there is a difference between them. The value of $13.25(\text{W}/\text{cm}^2)$ is observed in case of 5.0V, $9.9 (\text{W}/\text{cm}^2)$ for 4.0V and $2.9(\text{W}/\text{cm}^2)$ for 3.5V. The decreased power spectral in case of 3.5V is due to the electric field which is increased in case of 5.0V compared to 4.0V and 3.5V. Therefore, more separation of hole and electron wave functions is privileged resulting in less hole and electron recombination. However, the carrier recombination is favored.

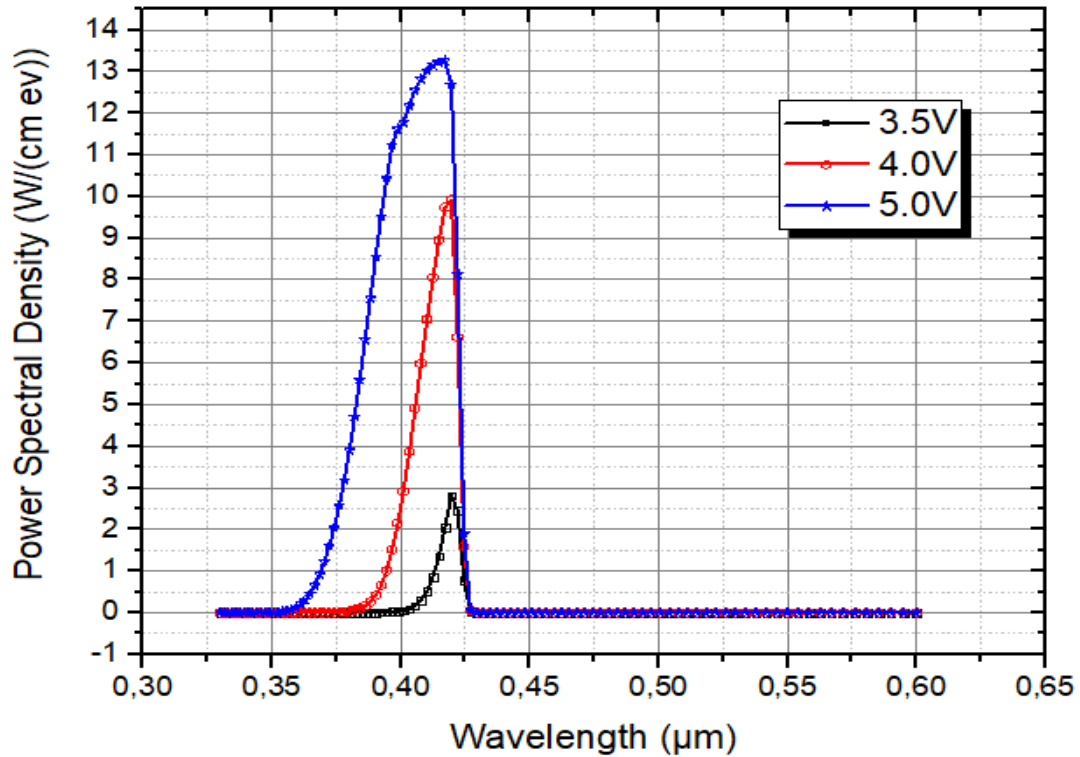


Figure III.13: The power spectral density of 2QWs for different bias voltage.

III.3.7. Internal quantum efficiency

Internal quantum efficiency (IQE) is given by the following formula:

$$\text{IQE} = \frac{\text{Recombinaison radiative}}{\text{Recombinaison totale}} \quad (\text{III.1})$$

Figure (III.14) shows the variation of the internal quantum efficiency (IQE) as function of the number of quantum wells.

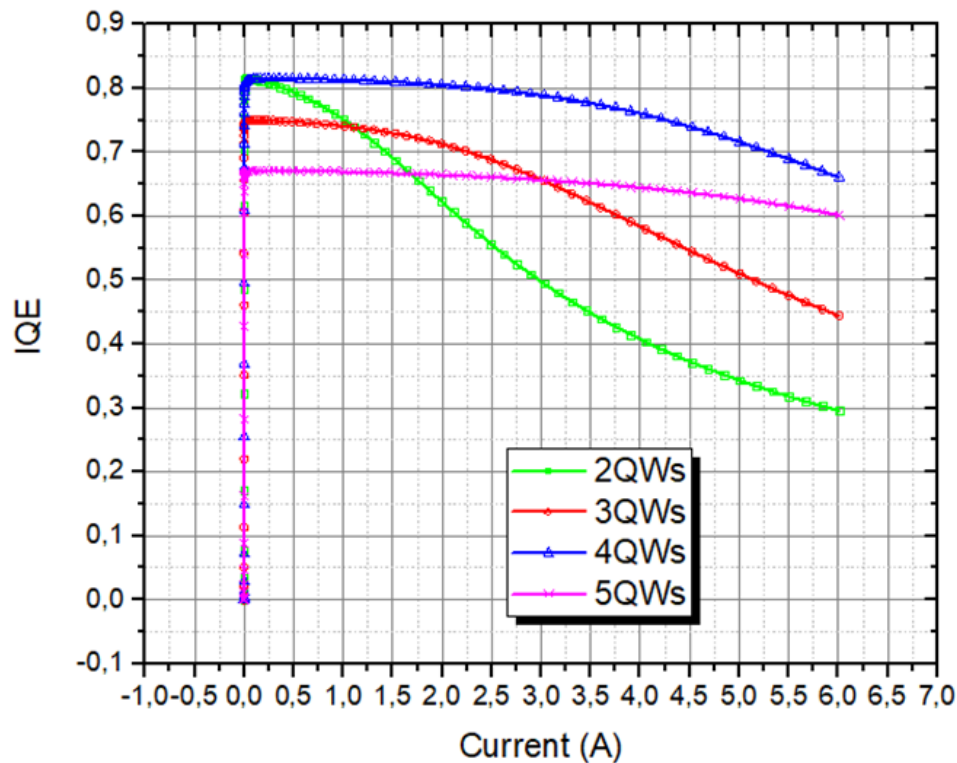


Figure III.14 Internal quantum efficiency (IQE) with number of wells.

Figure (III.14) shows that the internal quantum efficiency of different quantum wells is constant at 0.8 because the LED current is equal to 0A. In addition, internal quantum efficiency, for a given electric current, decreases every time the number of quantum wells rises, This is due to the rate of radiation recombination, which itself follows the same behavior with regard to electrical current as internal quantitative efficiency. The equation (III.1) confirms these latter observations. But also we can observe that as we increase the number of quantum wells above five efficiencies is again reduced, this may be attributed to the increase in radiative recombination rate caused due to the lower mobility of holes as compared to electrons which are not able to reach the well present on the n-GaN side. In addition, we notice a decrease in efficiency with increasing current density, the reason may be attributed to carrier overflow or less number of carriers being captured resulting in radiative recombination. If the number of quantum wells is reduced, the total number of carriers being captured in the well region is reduced and hence the radiative efficiency is reduced. This implies that one should have a high number of quantum wells to capture more and more carriers for recombination.

III.3.8. Comparison of ordinary and multiple quantum well light-emitting diodes

In order to compare an ordinary LED (single quantum well structure) to the 2QWs LED, both designs are simulated and studied using Silvaco-Atlas software. Figure (III.15) shows I-V characteristics of both 2QWs and single quantum well LEDs. This latter is simulated with 2.5 nm well width. It is clear that the 2QW LED structure indicates high turn on voltage compared to that of single quantum well LED, where a threshold voltage is 3.25V and 3.50V for SQW and 2QW LED, respectively. This is can be explained by the number of carriers which can be confined and captured in case of 2QW resulting in radiative recombination.

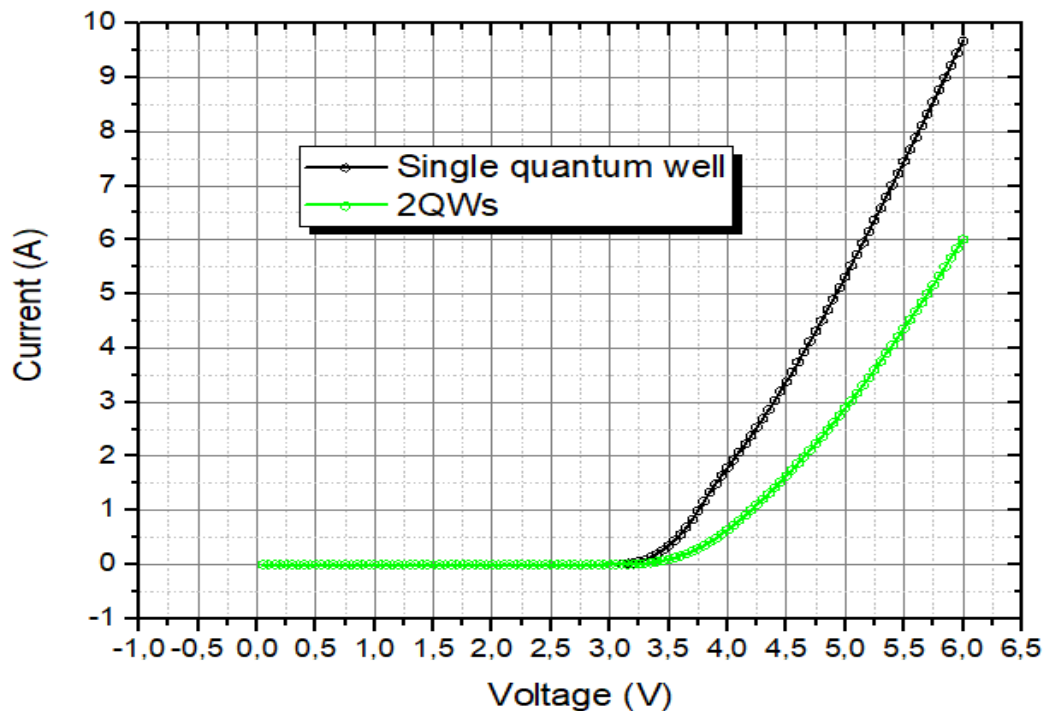


Figure III.15: I-V characteristics of SQM and 2QWs.

Figure (III.16) illustrates the variation of luminous power as a function of anode current. It presents increasing of luminous power for both structures. Accordingly, the high current delivered by SQW design resulting in high luminous power compared to the two quantum wells design.

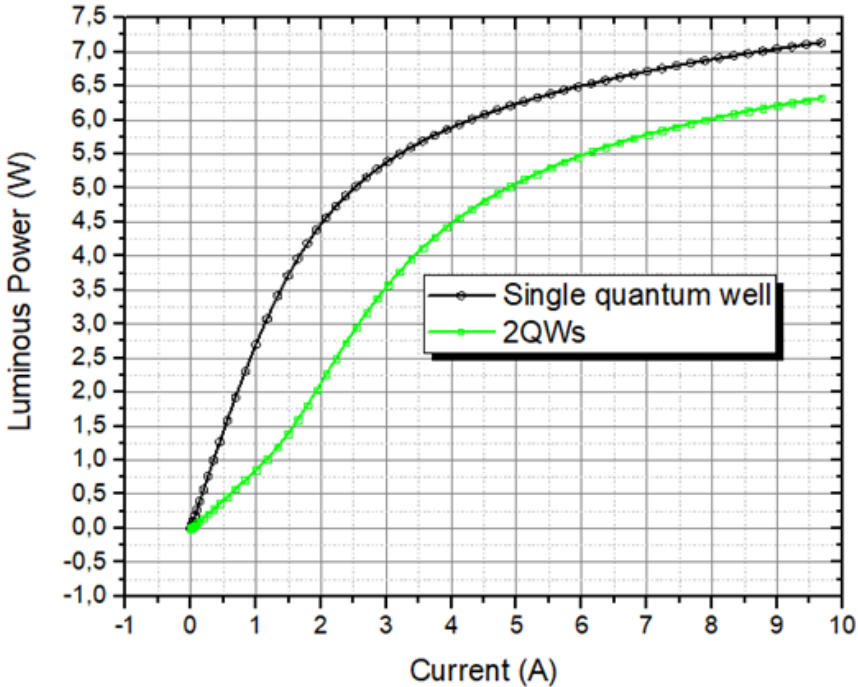


Figure III.16: Variation of Luminous power versus anode current.

General conclusion

The light emitting diode is an increasingly used component in various fields such as lighting, television screens, computer screens or decoration. It can replace traditional light sources. In this work, we have simulated an InGaN quantum well-based light emitting diode with a thickness of about 2.5 nm sandwiched between two layers of GaN doped respectively N and P. This sandwich confines in the active region, both electrons and holes thus increasing radiative recombinations. Using the SILVACO-ATLAS simulation software, we have studied the effect of the quantum well on the different recombinant mechanisms, the current-voltage characteristic (I-V), the spectral power, the optical power -current characteristic (P-I) and internal quantum efficiency for QWs LED. We can conclude our work on the following points:

- Each increasing in the number of quantum wells increases the turn on voltage.
- When the number of quantum wells decreases spectral power is better and the half-width of the spectral power increases.
- Luminous power is also good when a fewer quantum well are used.
- Compared 2QWs LED to 3QWs, 4QWs and 5QWs LEDs; we found that 2QWs LED was better than the rest.
- Single quantum well LED structure shows high current density and high luminescent power compared to that of 2QW LED structure.

REFERENCES

- [1] GRUNDMANN, Marius. Physics of semiconductors. Berlin : Springer, 2010.
- [2] FAZIA, Bouaraba. Etude d'une LED à base d'InGaN pour l'émission de la lumière blanche. Mémoire magister, Université Mouloud Mammeri de Tizi-Ouzou, 2012.
- [3] MAY, Gary S. et SPANOS, Costas J. Fundamentals of semiconductor manufacturing and process control. John Wiley & Sons, 2006.
- [4] م. قعقع، "الإلكترونيات الأساسية"، جامعة دمشق، دمشق، ص 301-314، 2015
- [5] BRENNAN, Kevin F. Introduction to semiconductor devices: for computing and telecommunications applications. Cambridge University Press, 2005.
- [6] MISHRA, Umesh K. et SINGH, Jasprit. Semiconductor device physics and design. Dordrecht: Springer, 2008.
- [7] SZE, Simon Min. Semiconductor devices: physics and technology. John wiley & sons, 2008.
- [8] LI, Sheng S. Semiconductor physical electronics. Springer Science & Business Media, 2012.
- [9] ROCKETT, Angus. The materials science of semiconductors. Springer Science & Business Media, 2007.
- [10] ا. الطاهر، ي. مصطفى، "مقدمة في فيزياء أشباه-الموصلات"، جامعة المنصورة، جامعة ام القرى، ص 161، 2017
- [11] MEKEMEICHE, Abdelkader. Etude à deux dimensions de cellules solaires en silicium monocristallin à émetteur sélectif à l'aide de PC2D. Thèse de doctorat, Université de Mostaganem-Abdelhamid Ibn Badis, 2013.
- [12] BENKHALED, Mohamed. Etude modélisation et simulation de l'effet des structures de faibles dimensions sur la conversion photovoltaïque. Mémoire magister, Université des Sciences et de la Technologie d'Oran Mohamed Boudiaf, 2019.
- [13] MECHAI, Fazia. Etude et simulation des structures photovoltaïques à base de chalcogénures de métaux de transition MX₂ (M= W, Mo; X= S, Se). Thèse de doctorat. Université Mouloud Mammeri, 2016.
- [14] Faycal Bouzid, « Simulation des propriétés électriques d'une jonction à base de nitrure de gallium. Application au détecteur de rayonnement », thèse de doctorate, Universete Mohamed Khider Biskra, 2018.
- [15] <https://www.azom.com/article.aspx?ArticleID=8466>
- [16] AMAR, Abdelhamid, RADI, Bouchaïb, et EL HAMI, Abdelkhalak. Influence de la couche de nucléation sur le comportement thermomécanique du HEMT. 2022.
- [17] Romuald Houdré, " Science et génie des matériaux", liver 2006 /2007.
- [18] FREYSSINIER, Jean Paul, ZHOU, Yutao, RAMAMURTHY, Vasudha, et al. Evaluation of

- light-emitting diodes for signage applications. In : Third International Conference on Solid State Lighting. SPIE, 2004.
- [19] MOTTIER, Patrick. LED for lighting applications. John Wiley & Sons, 2010.
- AMADOR-MÉNDEZ, Nuño. Nanostructured III-nitride light emitting diodes. Thèse de doctorat. université Paris-Saclay. 2022.
- [20] AMADOR-MÉNDEZ, Nuño. Nanostructured III-nitride light emitting diodes. Thèse de doctorat. université Paris-Saclay.2022.
- [21] A. Barlier-Salsi, M.A. Gautier, D. Brissinger, J.M. Deniel, Diodes électroluminescentes : risques pour les travailleurs exposés à la lumière bleue. INRS,2020.
- [22] WINDER, Steve. Power supplies for LED driving. Newnes, 2016.
- [23] HELD, Gilbert. Introduction to light emitting diode technology and applications. CRC press, 2016.
- [24] KASAP, Safa O. Optoelectronics and photonics: principles and practices. 2001.
- [25] AMINA, BALI. Etude comparative entre les cellules solaire de type p-AlGaAs/p-GaAs/n-GaAs et une autre de type n-AlGaAs/n-GaAs/p-GaAs. Magister en physique, UNIVERSITE MOHAMED KHEIDER-BISKRA.
- [26] POUSSET, Nicolas. Caractérisation du rendu des couleurs des nouvelles sources: les diodes électroluminescentes (LED). Thèse de doctorat. Conservatoire national des arts et métiers. 2009.
- [27] BELAID, Asma. Simulation et optimisation d'une diode électroluminescente B (Ga, Al) N/GaN émettant dans l'ultraviolet. Thèse de doctorat. 2020.
- [28] <https://www.motorscaffe.com/2022/11/Light-Emitting-Diode.html>
- [29] <https://www.electronpashaa.com/2023/04/Infrared-LED-Diode.html>
- [30] SCHUBERT, E. Fred, " Light-emitting diodes", Cambridge university press, 2006.
- [31] https://spie.org/publications/fg11_p26_light_emitting_diodes
- [32] RAMI, Boumaraf, "Simulation of the temperature and the deep traps effect on the electrical characteristics of GaAs diodes", Thèse de doctorat, Université de Biskra.
- [33] BEDDIAFI, Yazid, "Modélisation d'un transistor MESFET en GaAs en utilisant le simulateur atlas-Silvaco", Thèse de doctorat, 2013.
- [34] ELBAR, Mourad, Etude par simulation numérique d'une cellule solaire en CIGS à multi-jonction par le logiciel Tcad-Silvaco", Thèse de doctorat, Université Mohamed Khider–Biskra, 2018.
- [35] IZZEDDINE, MALLEM, "Simulation des cellules solaires hétérojonction Si-SiGe par Silvaco", Thèse de doctorat, 2014.
- [36] MANUAL, ATLAS User's, Device simulation software, Silvaco Int., Santa Clara, CA, 2008.
- [37] MAROUF, Yacine, "Modélisation des cellules solaires en InGaN En utilisant Atlas

Silvaco'', Thèse de doctorat, 2013.

- [38] BELARBI, M., “Étude à deux dimensions et optimisation des paramètres physiques et géométriques de cellules solaires de divers contacts interdigités”, Thèse de doctorat, université de Abd Hamid Ibn badis, Mostaganem. 2016.
- [39] MENACER, Fouzia. “Simulation des cellules solaires en InGaN en utilisant Atlas Silvaco'', Thèse de doctorat. Université Mohamed Khider–BISKRA. 2016.